2017-01-01

Biochemical characterization of wild-type Hsp27 and point mutation S135F that leads to neurodegenerative disease

Janelly Villalobos
University of Texas at El Paso, janellyvillalobos@gmail.com

BIOCHEMICAL CHARACTERIZATION OF WILD-TYPE HSP27 AND POINT MUTATION S135F THAT LEADS TO NEURODEGENERATIVE DISEASE

JANELLY VILLALOBOS

MASTER'S PROGRAM IN ENVIRONMENTAL SCIENCE

APPROVED:

Ricardo A. Bernal, Ph.D., Chair

Chu-Young Kim, Ph.D.

Kyung-An Han, Ph.D.

Charles Ambler, Ph.D.
Dean of the Graduate School

Dedication

To my family

BIOCHEMICAL CHARACTERIZATION OF WILD-TYPE HSP27 AND POINT MUTATION S135F THAT LEADS TO NEURODEGENERATIVE DISEASE

by

JANELLY VILLALOBOS, B.S.

THESIS

Presented to the Faculty of the Graduate School of
The University of Texas at El Paso
in Partial Fulfillment
of the Requirements
for the Degree of

MASTER OF SCIENCE

Department of Environmental Science
THE UNIVERSITY OF TEXAS AT EL PASO
December 2017

Acknowledgements

I would like to express my sincere gratitude to my mentor, Dr. Ricardo Bernal, for the continuous support in my two years of graduate school. His guidance and encouragement has been a tremendous help in this journey. Not only did he motivate us but pushed us to achieve our true potential. I could not have imagined having a better mentor for my Master's study.

Secondly, I would like to thank my colleagues, who became my second family. I thank all of them for the late nights we spent in the lab, for the challenges we faced together, for motivational words we shared, and finally the support we all had for each other through the good and the bad times.

I also like to thank my committee members: Dr. Han and Dr. Kim for being part of my last journey in graduate school, for their support and valuable time. Also for their insightful comments and questions that incented me to widen my research from various perspectives.

Lastly, I would like to thank my family for supporting me through my academic career. My best friends for providing me with unfailing support and continuous encouragement throughout my years of study. This accomplishment would not have been possible without everyone who supported me. Thank you.

Abstract

HSPB1, also classified as heat shock protein 27 (Hsp27), is a small chaperone that is active in cells during stressful conditions. The chaperone can stabilize target proteins in a non-aggregated folding state and might be involved in regulation of folding and assembly of neurofilaments. There are five mutations in the genome of Hsp27 that are involved in Charcot Marie Tooth Disease (CMT). This neurodegenerative disease is characterized by the first decades of life where it slowly progresses to weakness of muscles followed by sensory loss and skeletal deformities. CMT is the most common hereditary neuromuscular disease, with an estimated rate of 1 in 2500 people in the United States. It is still not clear what role the mutations play in the mechanism that leads to the disease. Some studies have shown that the mutations result in an abnormal binding affinity between the mutant and wild-type protein.

This project aims to study the function and structure of the wild-type Hsp27 compared to one of the mutations S135F. The gene for Hsp27 was cloned and transformed into BL21(DE3) bacterial cells for protein expression. It was then purified using anion exchange chromatography followed by size exclusion chromatography. The chaperone protein activity in the oligomerization state was assayed by using alpha-lactalbumin aggregated by a reducing agent, dithiothreitol (DTT) *in-vitro*. The secondary structure of Hsp27 WT and mutation S135F were evaluated through the following biophysical analyses: circular dichroism and dynamic light scattering. The structure of mutation S135F was evaluated under a transmission electron microscope.

Table of Contents

List of Figures

Chapter 1: Introduction

1.1 The Function and Structure of Proteins

Protein molecules are vital to any living organism. Proteins are built from a universal base set of 20 amino acids that are covalently linked together that are able to interact with each other to guide protein-folding, therefore, influencing function and overall size (Adams, 2008). The interactions that occur between the different amino acids has to be precise in order for the protein to maintain its correct function and structure. Improper folding can lead to a malfunction in the cells which leads to disease. Many studies are conducted on how function and structure of proteins change when a single amino acid is altered (i.e. point mutations).

1.1.1 Protein Biosynthesis

Proteins are involved in many roles such as catalyzing reactions, transporting molecules, and providing structure in order to maintain homeostasis in living organisms (Adams, 2008). Since proteins are extremely vital to a cell they must be continuously synthesized. The process begins with DNA replication in the nucleus of a cell, the DNA product is then transcribed into messenger RNA (mRNA). After transcription, the mRNA molecule exits the nucleus and moves into the cytoplasm where a ribosome begins to read the mRNA sequence. The ribosome recognizes three letter combinations known as codons that code for a certain amino acid. As amino acids are added to the chain of a growing polypeptide the nascent protein exits the ribosome and the folding process begins.

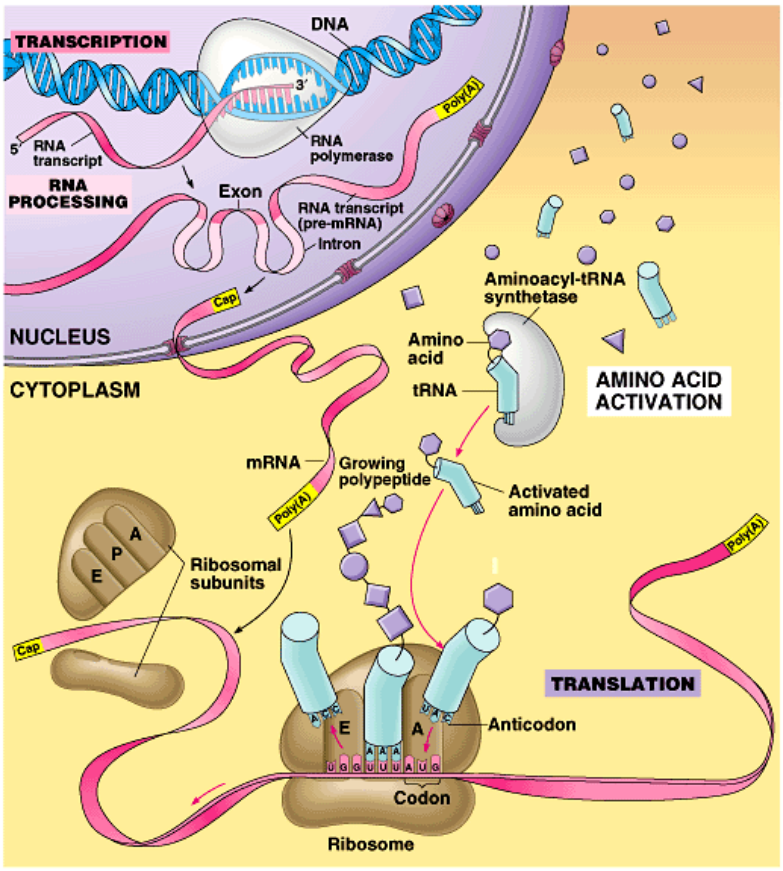

Figure 1.1 A summary of transcription and translation in eukaryotic cells. Adapted from Pearson Education, Inc., publishing as Benjamin Cummings (Cummings, n.d.).

1.1.2 Protein Structure Levels

Linderstrøm-Lang performed many laboratory studies on protein denaturation and the accessibility of peptide bonds and found that protein structure is highly dynamic (Schellman & Schellman, 1997). He and Schellman realized that protein structure was hierarchical and proposed four levels of complexed structural organization: primary, secondary, tertiary, and quaternary structure (Linderstrøm-Lang & Schellman, 1959) (Figure 1.2). All four levels that would play an important role in studying the function and structure of proteins.

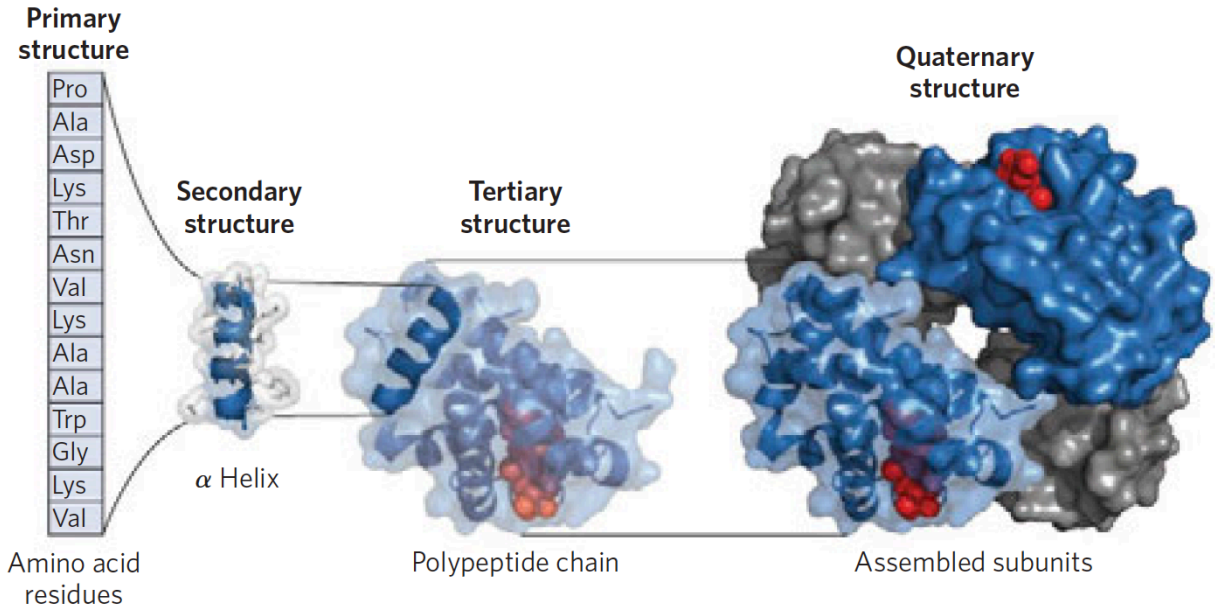

Figure 1.2 The primary structure consists of a sequence of amino acids linked together by peptide bonds. The polypeptide can be arranged into units of secondary structure, such as an alpha helix or beta strand. The units are part of the tertiary structure, and multiple subunits of itself make up the quaternary structure. Adapted from Lehninger Principles of Biochemistry, 6th Edition (Nelson & Cox, 2012).

The primary structure is a sequence of amino acids linked by peptide bonds that determines the architecture of how the protein will fold and function. The side chains of amino acids have different chemistries in terms of charge, polarity, and aromaticity. The chemistry within the amino acids is critical to protein structure because the unique side chains interact with one another, forming different kind of interactions (eg. hydrogen and covalent bonds, ionic and hydrophobic interactions) leading to a certain protein conformation that will determine how it functions. Therefore, the location of each amino acid is highly important for determining how a protein will bend and fold.

Secondary structures such as alpha helices and beta sheets are formed by the interactions of amino acids that from hydrogen bonds between each other. The secondary structure are hydrogen bonding patterns that give rise to helix and sheet

elements that are within a protein. Hydrogen bonding can only occur between hydrogen and a strong electronegative atom such as fluorine, oxygen, and nitrogen. Pauling and Corey proposed that these interactions were the building blocks of proteins defined by hydrogen bonding of close or distant related regions of the polypeptide chain (Pauling & Corey, 1951). The alpha helix presents itself as a rod-like structure where the inner section is composed of tightly coiled chains while its side chains are extending outward. The alpha helical structure is stabilized by hydrogen bonding between the amide hydrogen and the carbonyl oxygen (Engelking, 2015). The beta strands are composed of a long range of interactions that form beta sheets (Caetano-Anollés, Wang, Caetano-Anollés, & Mittenthal, 2009) (Engelking, 2015). The sheets can arrange in parallel when the two chains are aligned in the same direction from the amino group and carboxyl group or antiparallel sheets when both chains have opposing directions (Engelking, 2015) (Caetano-Anollés, Wang, Caetano-Anollés, & Mittenthal, 2009). There are different environments where a certain type of pattern may favor or maintain a better stability for the overall protein structure.

The tertiary structure is the overall three-dimensional structure of a protein. The folds are involved by using the lowest energy conformations of individual amino acids and forming a compact structure (Caetano-Anollés, Wang, Caetano-Anollés, & Mittenthal, 2009). The packing is composed of both alpha helix and beta sheets together where the side chains interact and maintain the structure (Caetano-Anollés, Wang, Caetano-Anollés, & Mittenthal, 2009) (Figure 1.3). For some proteins, they are made up of a single polypeptide chain and only have three levels of structure. However, other proteins can be made up of separate polypeptide chains that are folded into a

supramolecular unit known as quaternary structure. Once the protein is fully folded, structural changes may still arise due to things like changes in the environment, interaction with other proteins, or modification by other proteins or molecules (eg. cofactors).

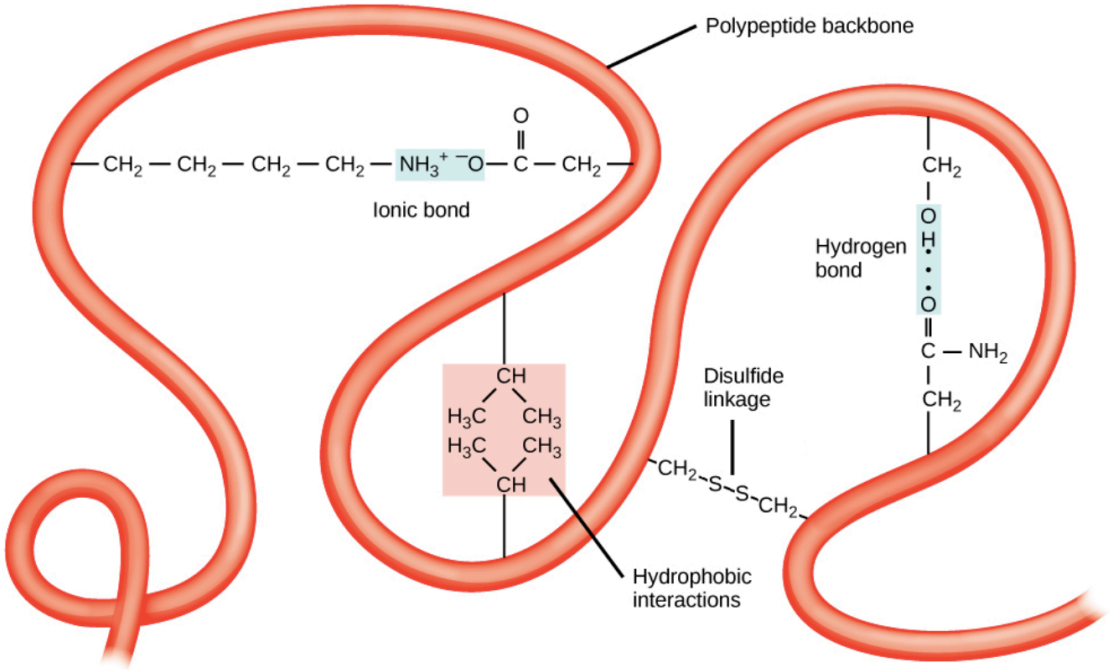

Figure 1.3 Represents the different interactions of amino acid side chains that contribute to tertiary structure. Some of the interactions include hydrogen bonding, ionic bonding, and dipole-dipole interaction. Also, hydrophobic interactions in which amino acids with nonpolar side chains cluster together in the inside of the protein, leaving the hydrophilic amino acids on the outside of the protein that can interact with other molecules. Another interaction are disulfide bonds, that are covalent linkages between the sulfur containing side chains of cysteines. This interaction is the strongest interaction that contributes to maintaining the tertiary structure because it keeps the polypeptide firmly attached together. Adapted from LibreTexts from bio.libretexts.org (Protein structure , 2017).

1.1.3 Chaperonins and Chaperones

Unfolded polypeptides can go through different conformations before finalizing to its final structure or native conformation. However, because the cytoplasm contains many organelles and a high concentration of proteins, there is a high risk of these proteins that are in the folding process to interact with other partially folded proteins (Alberts, et al.,

2013) (Evstigneeva, Solov'eva, & Sidel'nikova, 2000), This can lead to the misfolding of the protein and aggregation. Therefore, cells maintain proteostasis (Figure 1.4) by the use of chaperones and chaperonins that prevent unintended folding patterns that can occur (Alberts, et al., 2013).

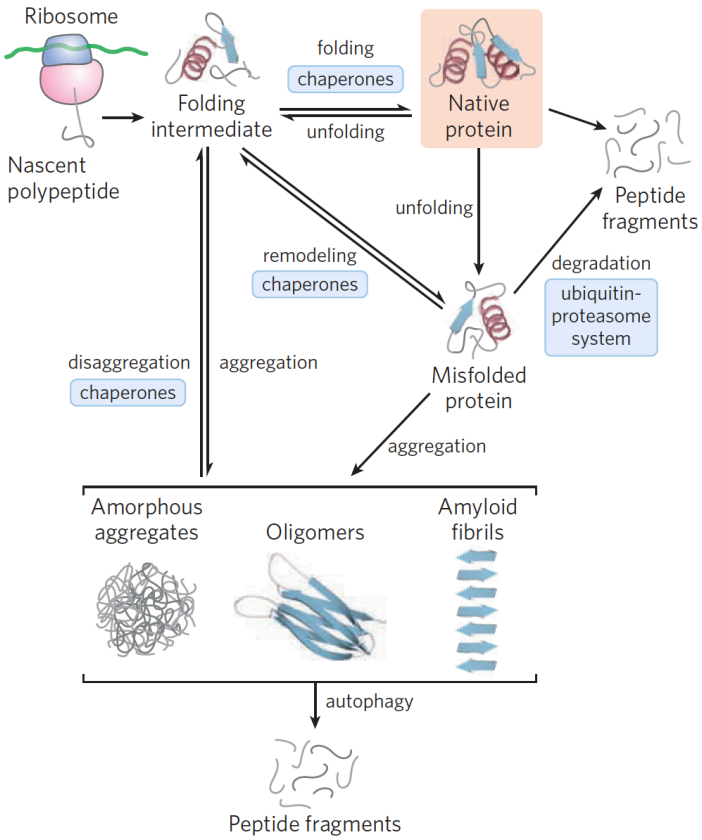

Figure 1.4 Three kinds of processes that contribute to protein homeostasis. Protein folding can go through different pathways with the assistance of a chaperones or chaperonins. With the help of a chaperone (including chaperonins), the protein can fold into its native conformation. If unfolding occurs, the protein becomes misfolded, which can aggregate, degrade, or go back to its folding intermediate. Adapted from Lehninger Principles of Biochemistry, 6th Edition (Nelson & Cox, 2012).

A chaperone is a protein that selectively recognizes and binds to proteins exposed hydrophobic surfaces in a noncovalent interaction in order to inhibit protein aggregation (Slavotinek & Biesecker, 2001) (Figure 1.5). Chaperones were discovered when there

was an increase of chaperone activity in cells during stressful conditions such as UV irradiation, temperature changes, and chemical challenges (Evstigneeva, Solov'eva, & Sidel'nikova, 2000). Because of this, chaperones are also called heat shock proteins (Hsp). All known chaperones have similar functions in that that they protect the protein from an environment that may cause the protein to aggregate.

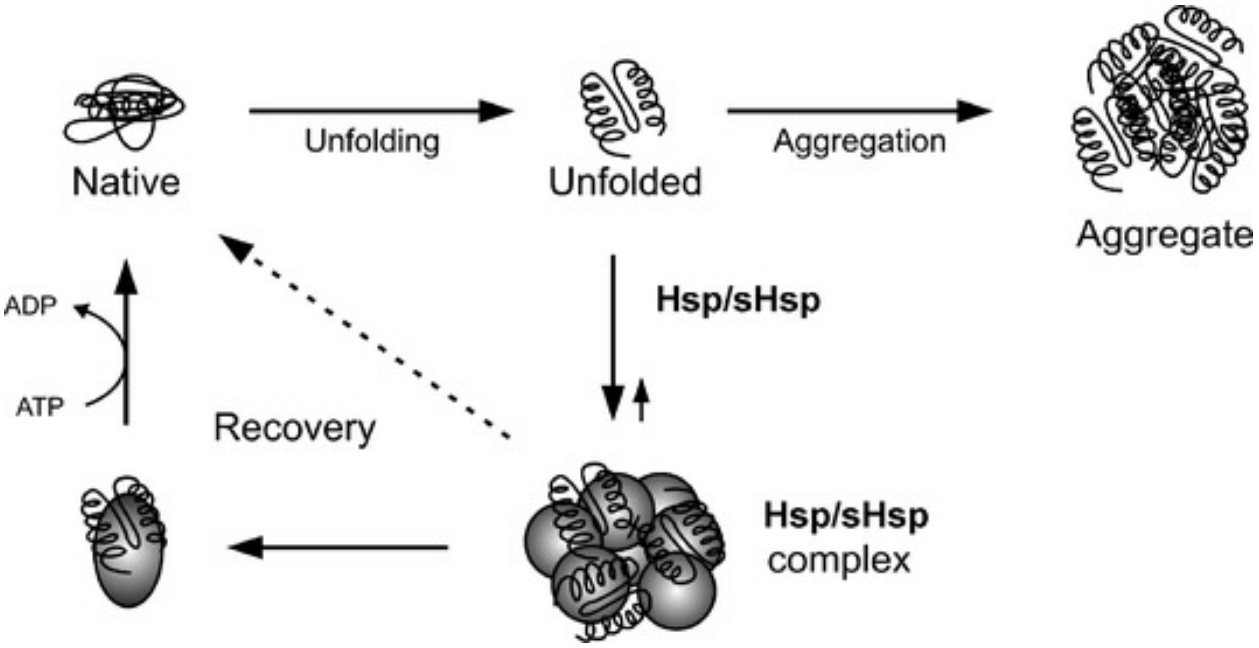

Figure 1.5 Represents the role of heat shock proteins and small heat shock protein in recognition and refolding of unfolded proteins. Heat shock proteins use ATP for folding proteins to their native conformation. If unfolded protein is not recognized by the Hsp/sHsp then the unfolded protein can form an aggregate. Adapted from Wilhelmus et al., 2007 (Wilhelmus, 2007).

There are two types of chaperones: the first is classified as monomers of 70-100 kDa, and the second group as chaperonins that have a complex oligomeric structure and a molecular weight of 800 kDa (Evstigneeva, Solov'eva, & Sidel'nikova, 2000). In the 1980s, Ellis proposed that chaperone protein families that have quaternary structure and high molecular weights are called chaperonins (Ellis, Phil. Trasn. Biol. Sci., 1993) (Ellis & Hemmingsen, Trends Biochem. Sci., 1989). The chaperonins are big complexes

composed of two stacked rings radially arranged subunits with a molecular weight of 60 kDa each (Slavotinek & Biesecker, 2001). These larger complexes are commonly ATP-dependent in folding non-native proteins and binding of non-native substrate (Bukau & Horwich, 1998). Their effective chaperonin activity is regulated by the binding of additional co-factors or co-chaperones that catalyze the inter-conversion between ATP and ADP states. When ATP binds to the chaperonin, it releases peptides rapidly, resulting in low overall affinity, whereas the ADP-bound chaperonin binds peptides slowly but more stably.

Chaperones, are small heat shock proteins that are ATP-independent, and are regulated by heat stress. Studies performed *in vitro* showed that small heat shock proteins work as molecular chaperones in preventing irreversible thermal denaturation of other proteins (Vierling, 1997). The hydrophobic surfaces of chaperones serve as the binding sites for a misfolded protein. This complex formation prevents protein aggregation until the polypeptide can be folded under favorable conditions (Slavotinek & Biesecker, 2001). Although the functions of chaperones and chaperonins have a similar principle, there is evidence that the assembly of a particular protein may be performed by a specific chaperone or chaperonin (Evstigneeva, Solov'eva, & Sidel'nikova, 2000).

1.1.4 Misfolded Proteins and their effect in Cellular Homeostasis

Proteins that are folded correctly, display specific biological activities whereas misfolded proteins can become detrimental to the cell (Evstigneeva, Solov'eva, & Sidel'nikova, 2000). Many neurodegenerative diseases have been linked to the accumulation of misfolded proteins turning into aggregated protein, or soluble protein gradually converted to insoluble protein (Selkoe, 2004). As the buildup of these misfolded

proteins occurs this progressively compromises the cellular and tissue function, leading to different diseases (Selkoe, 2004).

Chaperones themselves can also become misfolded due to mutations within their encoding can gene, physical or chemical changes. This can quickly become problematic because a misfolded chaperone can no longer aid in the prevention of aggregation of other misfolded proteins. Chaperones that are deficient because of a structural change, may result in the formation of defective proteins that are no longer transported to appropriate subcellular destination, or that exhibit a loss-of-function (Ellis, Proteins as molecular chaperones, 1987) (Hohn, Hohn, Engel, Wurth, & Smith, 1979) (Hartl, 1996) (Langer, et al., 1992). This can be seen in many diseases such as Desmin-related myopathy, Congenital cataracts, and Charcot Marie Tooth (CMT) (Slavotinek & Biesecker, 2001).

1.2 The Molecular Chaperone Heat Shock Protein27

The gene HSPB1 encodes for the small heat shock protein 27 (Hsp27) that is a systemically expressed molecular chaperone that can be located in the brain, smooth, skeletal, and cardiac muscles. Hsp27 is a member of the small heat shock proteins found in both prokaryotic and eukaryotic cells. Hsp27 is part of the alpha crystallin family because it shares a conserved 80-100 amino acid sequence (Haslbeck, 2002) (Fontaine, Rest, Welsh, & Benndorf, 2003). The protein is composed of 205 amino acids with a molecular mass of 27 kDa as the name implies.

1.2.1 Quaternary Structure of Hsp27

Many small heat shock proteins share a common architecture arising from the conserved alpha-crystallin domain (ACD), proposing that this location has an important role in the assembly of the final structure (Baranova, et al., 2011). Scientific papers have reported that truncated ACD mediates a dimer formation of individual units that may assemble the arrangement of small heat shock proteins (Baranova, et al., 2011). This dimer is formed by the symmetrical antiparallel pairing of two beta-strands (beta7), generating an extended beta-sheet on one face of the ACD (Baranova, et al., 2011). However, the ACD fragment in Hsp27 shows hexamers (six structural subunits) by an asymmetric contact between beta4 and beta7 strands from adjacent ACDs (Baranova, et al., 2011). A crystal structure, showed a relative weakness of this interface (beta7/beta7 and beta4/beta7) that can easily dissociate and rearrange (Baranova, et al., 2011). Therefore, it could easily come apart by a point mutation present in the ACD which may explain diseases that are caused by structural effects in heat shock proteins.

The structure of ACD seems to be a hotspot for many diseases causing inherited mutations (Sun & MacRae, 2005), (Laskowska, Matuszewska, & Kuczyńska-Wiśnik, 2010). Six missense mutations located in the ACD of Hsp27 have been linked to type II form of Charcot-Marie-Tooth neuromuscular disease and distal hereditary neuropathy (Laskowska, Matuszewska, & Kuczyńska-Wiśnik, 2010) (Dierick, Irobi, De Jonghe, & Timmerman, 2005). However, the structure of Hsp27 and other small heat shock proteins remains unknown because they form heterogeneous structures due to the polydispersity of ACD. Recent crystal structures of the ACD containing fragments from

several vertebrate sHsp's reveal a lack of pattern in the dimer interface (Bagnéris, et al., 2009) (Laganowsky, et al., 2010).

Many have reported that the structure of Hsp27 is yet to be discovered due to the range of oligomerization states (Mymrikov, Bukach, Seit-Nebi, & Gusev, 2010) (Almeida-Souza, et al., 2010). The quaternary structure of Hsp27 can form a range of oligomers, from dimers of an estimated size of 54 kDa, to large complexes of about 800 kDa (Takeuchi, 2006). It is said that there is a dynamic process between the formation of dimers, tetramers, and oligomers. The oligomers can consist of 16 to 32 subunits that are exchanged within each other at a high rate (Thériault, et al., 2004), (Ehrnsperger, Lilie, Gaestel, & Buchner, 1999) (Rogalla, et al.). The complex of Hsp27 is regulated upon phosphorylation by mitogen-activated protein (MAP)-kinase-dependent (MAPKAPK2) (Garrido, et al., 1999), which leads to the dissociation of the complex. The range of subunit exchange and formation of different sizes, gives rise to its unique functions within the cell.

1.2.2 Function of Hsp27

Hsp27 is upregulated in times of cellular stress and limits the consequences of cellular damage by increasing cellular recovery rates. In response to environmental, physical, and chemical changes, Hsp27's primary function as a chaperone is to recognize and bind to exposed hydrophobic patches of partially denatured proteins, preventing them from irreversible aggregation. Many of the charged residues in Hsp27 are critical for chaperone functions, but difficult to identify if specific residues are involved in substrate binding and loss of chaperone function. The unfolded substrates are kept in a folding competent state until they can be shuttled to a chaperonin complex

for refolding or are marked for degradation. Hsp27 can interact with diverse substrates as a general chaperone preventing the aggregation-prone misfolded proteins from interacting. Notably, Hsp27 binds to signal transduction proteins with a number of transcriptional factors and mRNA processing proteins such as mRNA splicing proteins (Marin-Vinader, Shin, Onnekink, Manley, & Lubsen, 2006) (Fu, 2014). Furthermore, Hsp27 has different chaperone functions dependent on the substrate and the oligomerization state (Arrigo & Gibert, 2012) (Katsogiannou, Andreieu, & Rocchi, 2014). Hsp27 undergoes a concentration-dependent equilibrium dissociation from large oligomers to a dimer. This phenomenon plays a critical role in the primary function of Hsp27 as a chaperone that mediates protein folding, enabling high affinity binding to destabilized client proteins (McDonald, Bortolus, Koteiche, & Mchaourab, 2012).

Hsp27 is not always depended upon for protein folding as it is also involved in various cellular roles such as control of apoptosis, regulation of actin dynamics, and protection against oxidative stress (Figure 1.6) (Arrigo, et al., 2005) (Aquilina, Shrestha, Morris, & Ecroyd, 2013).

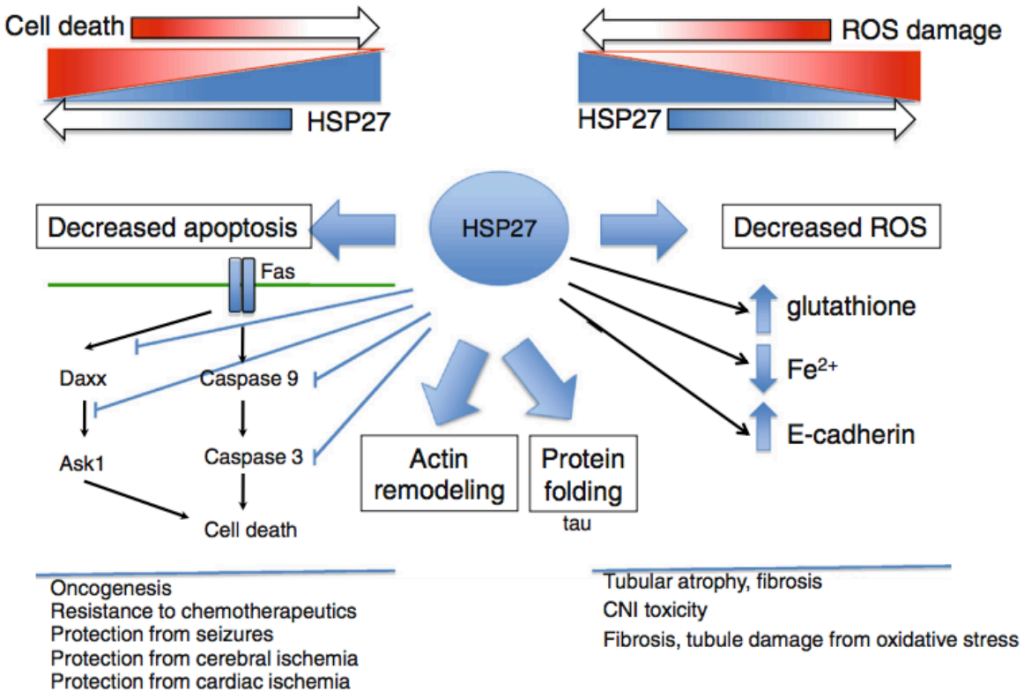

Figure 1.6 A summary of the main mechanisms of Hsp27. The primary mechanism is protein folding, effects on the cytoskeleton, reduction of oxidative stress, suppression of apoptosis or cell death. Hsp27 presents in various oligomeric states and is regulated by phosphorylation. Adapted from Vidyasagar et al, 2012 (Vidyasagar, Wilson, & Djamali, 2012).

Several investigations revealed that Hsp27 responds to cellular stress conditions other than heat shock; for example, chemical and oxidative stress. During oxidative stress, Hsp27 functions as an antioxidant by increasing the levels of glutathione and decreasing the levels of iron that is essential to reactive oxygen species (ROS) formation (Vidyasagar, Wilson, & Djamali, 2012) (Arrigo, et al., 2005) (Mehlen, Hickey, Weber, & Arrigo, 1997). Hsp27 also functions as an anti-apoptotic agent in chemical stressed environments by interacting with mitochondrial dependent and independent pathways. Interestingly, the protein can protect the cell from stress-damage-induced death by inhibition of caspase-dependent apoptosis (Vidyasagar, Wilson, & Djamali, 2012) (Calderwood, Khaleque, Sawyer, & Ciocca, 2006) (Takeuchi, 2006) (Charette, Lavoie, Lambert, & Landry, 2000) (Charette & Landry, 2000). Previous studies reported

that high expression levels of Hsp27 can be found in many cancers such as leukemia, breast cancer, and endometrial cancer (Fuller, et al., 1994) (Ciocca, Oesterreich, Chamness, McGuire, & Fuqua, 1993). Lastly, Hsp27 has the ability to regulate actin cytoskeletal dynamic during heat shock and other stress conditions (Benndorf, et al., 1994) (Huot, Houle, Spitz, & Landry, 1996). The regulation relies on phosphorylated Hsp27 where it prevents filament degeneration and promotes polymerization (Guay, et al., 1997) (Huot, Houle, Spitz, & Landry, 1996), whereas unphosphorylated Hsp27 acts as an actin capping protein (Benndorf, et al., 1994).

1.3 The Role of Hsp27 in Charcot-Marie-Tooth Disease

Charcot-Marie-Tooth (CMT) disease is a disorder that affects the peripheral nervous system causing weakness and atrophy of distal limb muscles, depressed or absent tendon reflexes, and mild to moderate sensory abnormalities (Charcot-Marie-Tooth Disease Fact Sheet, n.d.). The disease affects 1 in 2500 people in the U.S. CMT is caused by mutations in genes that produce proteins that are involved in the structure and function of the peripheral nerve axon and the myelin sheath (Charcot-Marie-Tooth Disease Fact Sheet, n.d.) (Charcot-Marie-Tooth Disease (CMT), 2017). The nerves begin to degenerate and lose their ability to send signals to distant targets. This results in muscle

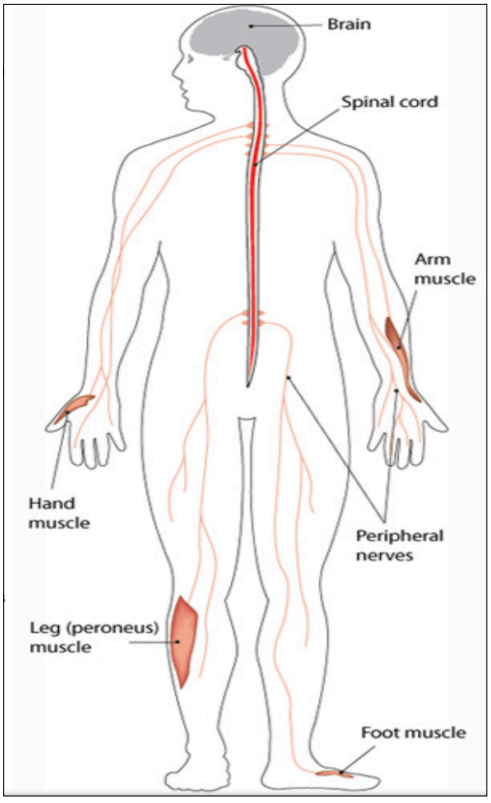

Figure1.7 CMT causes degeneration of the peripheral nervous system, leading to muscle weakness in the body's lower extremities (Charcot-Marie-Tooth Disease (CMT), 2017).

weakness in the arms, legs, hands, or feet (Figure 1.7). The disease is commonly inherited in an autosomal dominant fashion, meaning only one copy of the abnormal gene is needed to cause the disease (Charcot-Marie-Tooth Disease Fact Sheet, n.d.).

There are many forms of CMT such as CMT2 that results from abnormalities in the axon of the peripheral nerve cell rather than the myelin sheath. There are less common forms of CMT2 that are associated with gene mutations in genes such as HSPB1, that encodes for Hsp27. In 2004, it was reported that five point mutations located in small heat shock protein 27 were linked to CMT and distal hereditary motor neuropathy. Interestingly, four of the five mutations are located in the alpha-crystallin domain, which can cause loss of chaperone activity (Muchowski, Wu, Liang, Adman, & Clark, 1999) (Chung, et al., 2008) (Evgrafov, et al., 2004). Three of these (S135F, R127W, and R136) mutations lead to an increase, rather than a loss in chaperone activity (Almeida-Souza, et al., 2011), whereas the other two mutations (T151I and P182L) do not show hyper activation. This could be due to mutations displaying an increased affinity to their client proteins (Almeida-Souza, et al., 2011), and therefore failing to release the misfolded protein.

Hsp27 can stabilize target proteins in a non-aggregated folding-competent state, and might be involved in the regulation of folding and the assembly of neurofilaments (Pareyson, Marchesi, & Salsano, 2013). *In vivo* studies found that mutation S135F in Hsp27 affects the filament networks by causing aggregates in the assembly of the neurofilaments leading to premature axonal degeneration (Evgrafov, et al., 2004). As highlighted, the exact role of each point mutation and whether its primary function in protein folding is the underlying cause in CMT remains unclear. A complete

understanding of all cellular processes explaining the pathogenesis and the structures of all point mutations in Hsp27 remains elusive.

Chapter 2: Methodologies in Structural Biochemistry

2.1 DNA Cloning

Molecular cloning is a process where a DNA of interest is introduced into a carrier DNA known as a plasmid that is transported into a host where many copies of recombinant DNA are reproduced (Nelson & Cox, 2012). There are several procedures involved in restriction enzyme cloning which was the cloning method used in this work (Figure 2.1): Cutting the target DNA at precise locations by using restriction endonucleases, selecting a cloning vector for delivery of the gene into the cells, joining the vector and the DNA through DNA ligase, moving the recombinant DNA to a host cell for reproduction, and finally identifying host cells that contain the DNA (Nelson & Cox, 2012). There are a variety of host cells that can be used to obtain recombinant protein, but here we focus on DNA cloning in *Escherichia coli* (*E. coli*).

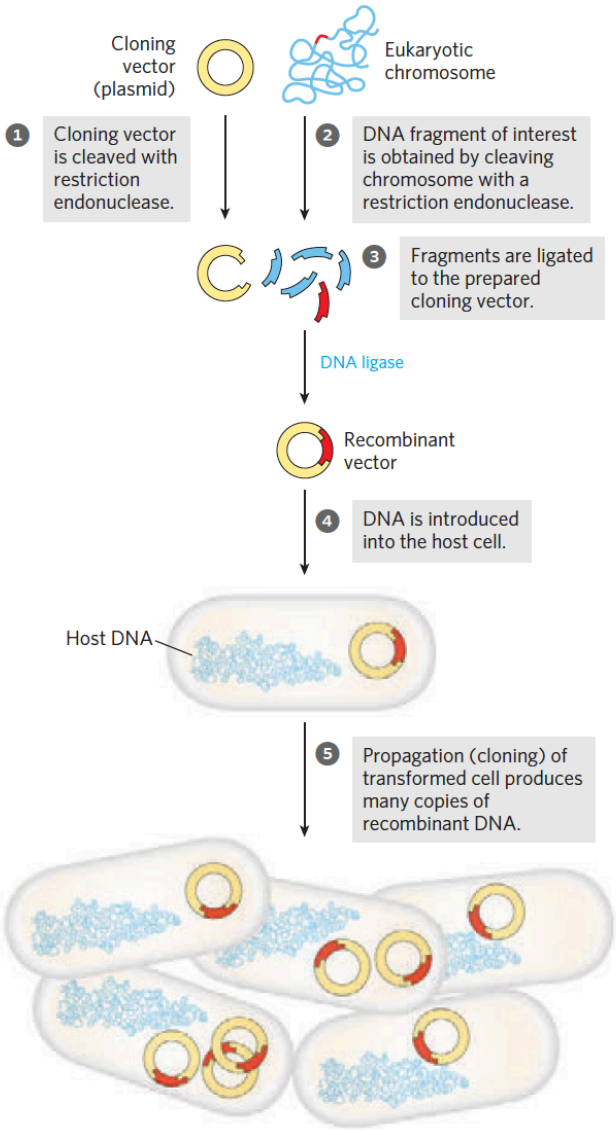

Figure 2.1 A schematic diagram showing the steps in cloning beginning with digestion of the vector and DNA through the use of restriction endonucleases, ligating the sticky or blunt ends of the vector and plasmid, followed by inserting the recombinant vector to a host cell, where the host cell produces many copies of recombinant DNA. Adapted from Lehninger Principles of Biochemistry, 6th Edition (Nelson & Cox, 2012).

2.1.1 Amplification of Gene Sequences through Polymerase Chain Reaction

Polymerase chain reaction (PCR) is a revolutionary technique developed by Kary Mullis in the 1980s. It is used to synthesize many copies of a specific DNA sequence. The process begins with designing oligonucleotides, short single stranded sequences of nucleotides, that complement approximately 18-24 bases at the 5' and 3' ends of the target DNA sequence for generating many copies of the gene. The reaction goes through a series of temperature changes that can allow certain reactions to occur (Figure 2.2). The reaction mixture is heated to 98ºC to denature double stranded DNA, and then cooled 60ºC-70ºC to allow the primers to bind to the 3' ends of the single stranded DNA. The primed segment is then replicated at 72ºC by a heat-stable DNA polymerase, that adds nucleotides to the preexisting strands. The cycles of heating, cooling, and replication are repeated 25 to 30 times over a few hours. The final product is many copies of the amplified DNA that can be readily used for cloning.

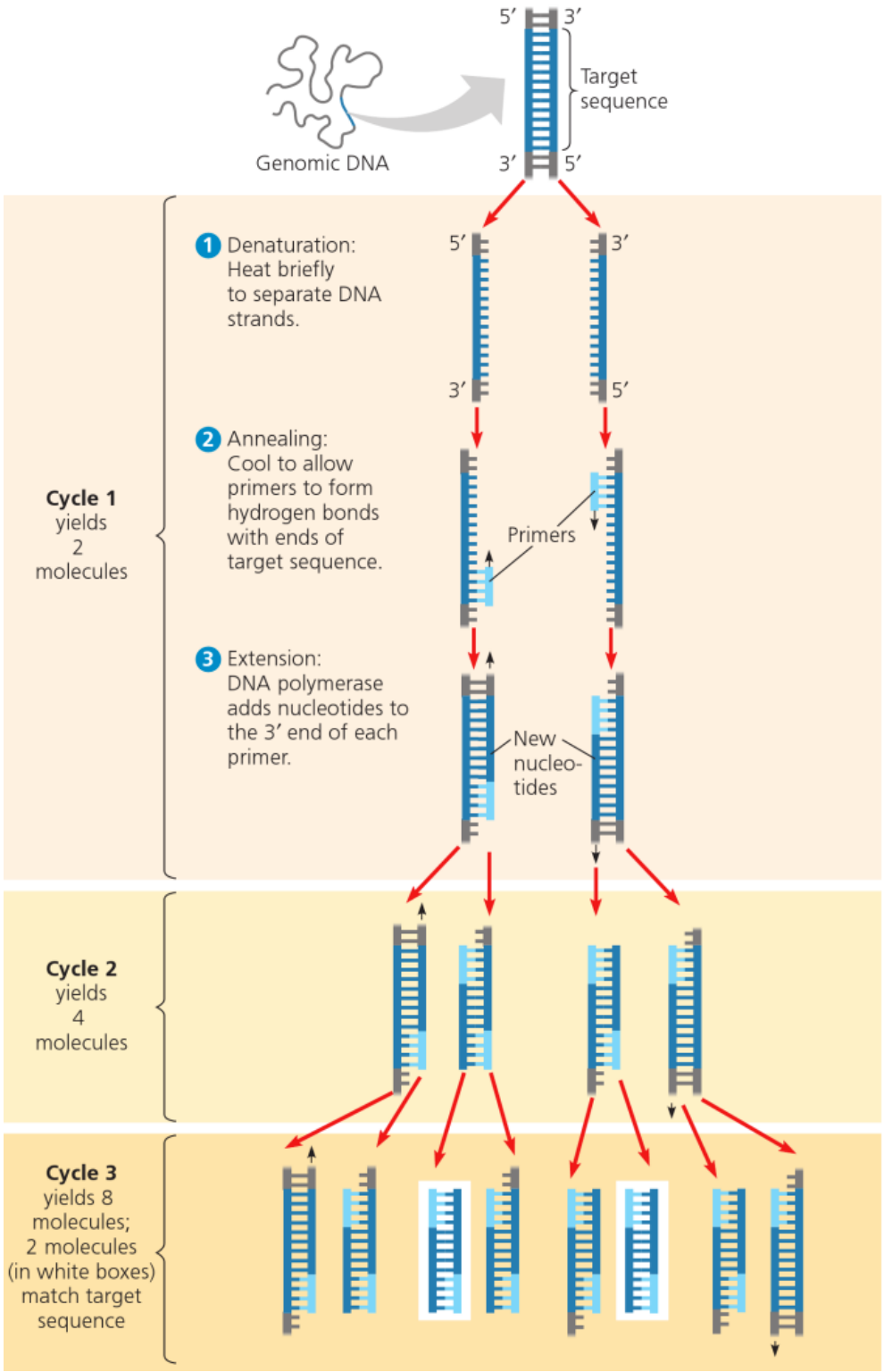

Figure 2.2 A schematic diagram of the cycles in the polymerase chain reaction with a final product showing many copies of the initial gene. Adapted from Giri, 2015 (Giri, 2015).

2.1.2 The Components of a Plasmid

A plasmid is a circular DNA that is used as cloning or expression vector each having their own properties to replicate inside the host organism (Figure 2.2). All vectors have an origin of replication sequence where replication is commenced by cellular enzymes. Another vital property is that plasmids contain genes that allow them to be resistant to some antibiotics such as ampicillin, permitting the selection of cells that contain the vector to survive and replicate. Another unique feature is the multiple cloning site that contains sequences for restriction endonuclease recognition where the plasmid can be cut to insert foreign DNA.

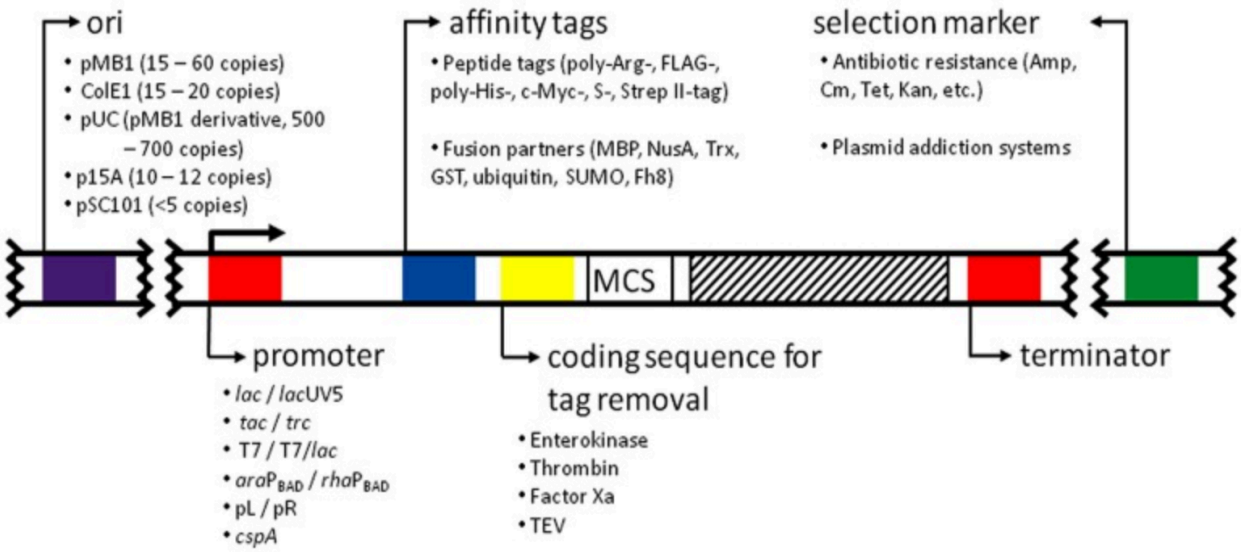

Figure 2.3 A map section of an expression vector system that contains a selection marker for antibiotic resistance. A multiple cloning site, an origin of replication that denotes how many copies are produced depending on the expression vector. Affinity tags and promoters that are recognized by some polymerases such as T7 polymerase. Adapted from Rosano & Ceccarelli, 2014 (Rosano & Ceccarelli, 2014).

2.1.3 Bacterial Transformation

Bacterial transformation is a step where bacterial cells uptake foreign genetic material through heat shock that is done by rapidly shifting the temperature. Bacteria that have the ability to take up exogenous DNA are termed competent cells. These cells contain calcium or other divalent cations that are bound to the cell membrane that attract and stabilize the negatively charged DNA to enter the cell. The bacterial membrane becomes permeable upon heat shock and takes up the plasmid DNA. The next step involves screening for cells that contain the plasmid by growing the cells in nutrient-rich medium (e.g. LB Agar) that contain the selectable marker in the form of an antibiotic. Cells that uptake the plasmid would have an antibiotic resistance factor that would select for survival against the antibiotic that is present in the media. Cells that do not have plasmid are susceptible to the antibiotic in the media and are therefore unable to propagate.

2.2 Protein Expression and Purification

2.2.1 Bacterial Expression of Recombinant Protein

Bacterial expression of recombinant proteins has given the opportunity for biochemists to produce high quantities of proteins. *Escherichia coli* is one of the most popular organisms for the production of recombinant proteins. The gene of interest is cloned into an expression vector, such as a pET system vector, then transformed into an expression host like BL21 (DE3), and finally the cells are grown in rich media where the protein is induced in the presence of lactose or lactose analogs. The strategy used for protein production is done by the modification of *E. coli's* genome to contain a copy of the T7 RNA polymerase found in bacteriophage T7. This polymerase results in the transcription and subsequent translation of the target gene (Figure 2.4). The process

begins with the lac repressor binding to the lac operator that regulates the promoter upstream of the gene encoding for expression of T7 polymerase. In the presence of an inducer, for example isopropyl β-D-1-thiogalactopyranoside (IPTG), an analog of lactose, binding to the lac repressor causes a conformational change that leads to the repressor falling off the operator resulting in the liberation of the promoter and concomitant production of T7 polymerase. In the pET vector system, the T7 RNA polymerase selectively binds to the T7 promoter, and upon removal of the repressor located upstream from the target gene by IPTG, transcription of the gene followed by translation occurs. (Figure 2.4). To control basal expression, glucose may be added to avoid leaky expression via regulation of the lac repressor.

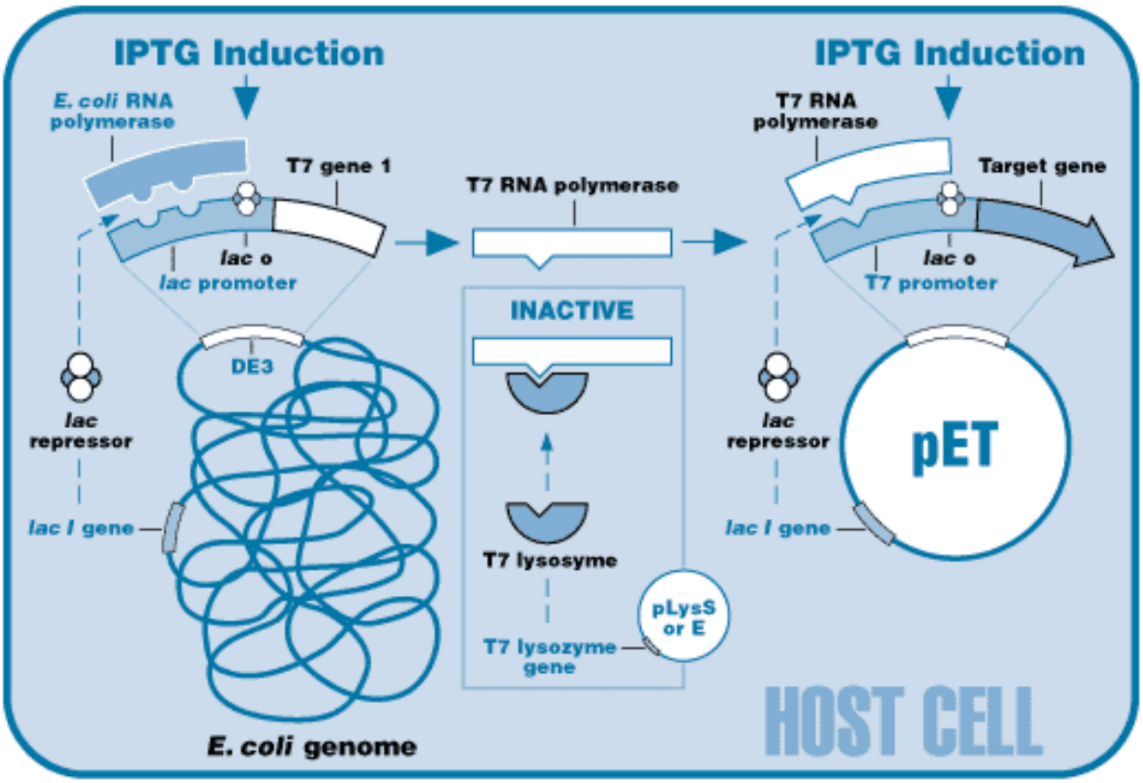

Figure 2.4 The regulation of transcription in a host cell for obtaining recombinant protein using T7 RNA polymerase and IPTG. Adapted from the pET Manual (PET system manual, n.d.).

The amount of recombinant protein obtained from the bacteria can result in high concentrations. However, some problems can occur, such as the cells not growing, inclusion body formation, protein inactivity, or not obtaining any protein. There are optimizations such as expressing protein at lower temperatures, using different concentrations of IPTG, using a different vector system, changing the media, or choosing promoters with tighter regulation. All of which can contribute to higher yields of protein.

2.2.2 Protein Extraction

The target protein is extracted from cells by following a variety of procedures that can either be physical or chemical in nature. Some of the procedures depend upon the isolation of the protein in terms of sample type, location of the protein of interest, the stability, and the required protein yield. Cells can be lysed through the following mechanisms: freeze thawing, sonication, pressure homogenization, osmotic and chemical lysis (Traditional methods of cell lysis , n.d.). Freeze-thaws is the gentlest procedure where multiple cycles of freeze-thaws cause the cells to swell as ice crystals form during the freezing process, allowing the cell wall to break. In addition, additives such as lysozyme and lysis buffer that contains EDTA, facilitate the process of physical disruption. EDTA is a chelating agent the sequesters divalent cations that support the stability of the outer membrane of gram-negative bacteria (Alakomi, Paananen, Suihko, Helander, & Saarela, 2006) (Alakomi , Saarela, & Helander, 2003) (Vaara, 1992) (Block, 2001). Lysozyme can then pass through the disrupted membrane, where it damages the glycosidic linkages that support the peptidoglycan.

As cells are lysed, the controlled environment the cell was initially in is disturbed, allowing endogenous proteases and phosphatases to become unregulated and result in

proteins that are degraded (Overview of cell lysis and protein extraction, n.d.). To prevent these effects, protease inhibitors such as AEBSF and PMSF are added to lysis reagents and the rest of the steps in protein extraction.

2.2.3 Fast Protein Liquid Chromatography

Fast protein liquid chromatography (FPLC) is a medium-pressure chromatography that was introduced in 1982 by Pharmacia (Fast protein liquid chromatography , n.d.). Since then many different medium-pressure chromatography systems have been improved and developed for purification of proteins. The system consists of a pump, a UV detector, conductivity meter, and a fraction collector (Figure 2.5). Some systems also have column switching valves and buffer blending valves to generate a gradient. Samples can either be loaded by injection into a sample loop or a sample pump.

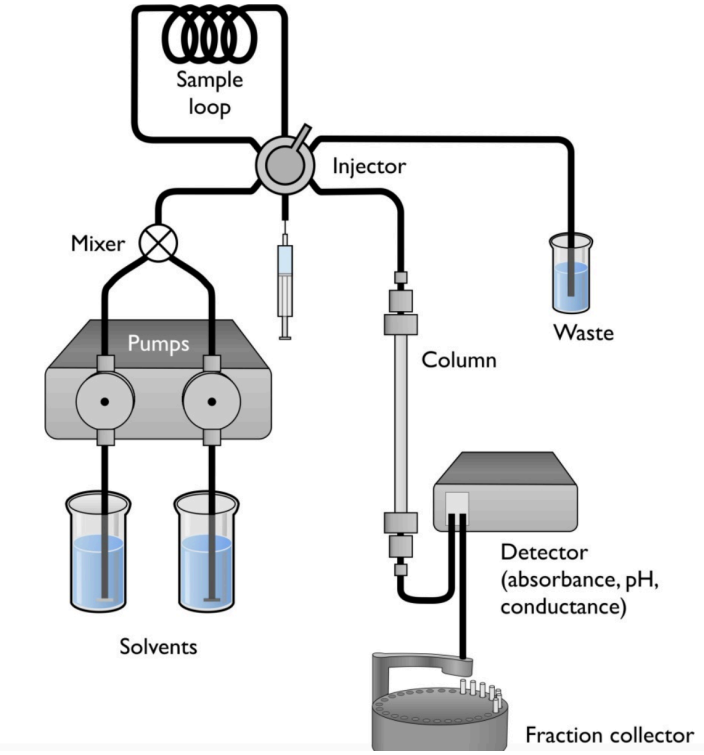

Figure 2.5 A schematic diagram of a liquid chromatography system, composed of a pump, mixer, sample application, a detector, and fraction collector. Adapted from Introduction to practical biochemistry (6.5 High performance (high pressure) liquid chromatography (HPLC), n.d.).

This technique is useful for separation of proteins based on their physical and chemical properties. The system works by the liquid mobile phase, or the buffer, passing through the column, where the molecules present in the buffer, are separated based on their physiochemical interactions with the stationary phase (resin) (Liquid chromatography principles, n.d.). Some of these interactions are based on molecular size, hydrophobicity, specific binding interactions, and charge interactions. Each type of interaction corresponds to columns that are purposely designed for these specific interactions between the protein and the resin.

2.2.3.1 Ion-exchange Chromatography

Ion-exchange chromatography is a type of column designed to separate proteins based on their total surface charge (Figure 2.6). To determine the overall surface charge, the isoelectric point (pI) of the protein is calculated based on the primary sequence of the protein (Ion exchange chromatography, n.d.). This value represents the pH at which the protein has no net charge. The choice of pH in the buffer determines the net charge of the protein of interest (Ion exchange chromatography, n.d.). For example, isolation of an isoelectric point that is 5.9 and a buffer with a pH of 7.5 would be carried out by using a positively charged resin column (anion exchange) due to the protein sample having a net negative charge, whereas an isoelectric point value that is higher than pH of 7 would be supported by a column with a negative charged immobilized group (cation exchange) where a positively charge protein can bind. The workflow of the ion exchange column after loading the crude sample, is done by washing the column with buffer that contains a low concentration of salt to washout weakly bound proteins or proteins that did not bind to the column. After this, the system is set up to elute the protein of interest based on a

salt gradient. As the charged salt ions pass through the stationary phase, the salt ions compete with bound proteins. Proteins with a low net charge would elute with low concentrations of salt, whereas proteins with many charged groups would or a high net charge elute with a higher concentration of salt.

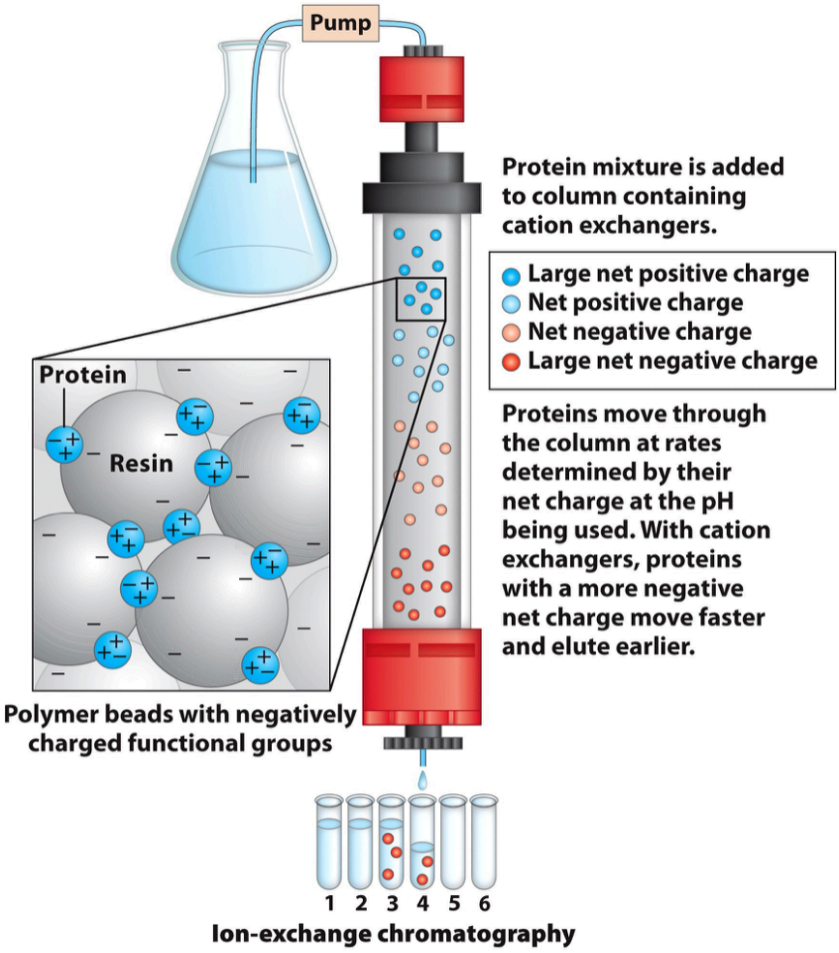

Figure 2.6 Ion exchange column composed of negative charged resin (cation exchange) bound with positive charged protein. Proteins that are net negatively charged cannot bind to the resin and are eluted earlier. Adapted from Lehninger Principles of Biochemistry, 6th Edition (Nelson & Cox, 2012).

2.2.3.2 Size-exclusion Chromatography

Size-exclusion chromatography is a column that is used to isolate molecules based on their size (Figure 2.7). There are a variety of size-exclusion columns that are composed of different pore sizes and column lengths (Introduction to size exlusion chromatography, n.d.). The pore size and column length contribute to the resolution of separated protein mixtures. Columns such as the superpose 6 increase has small spherical bead size of 8.6 μM that results in higher purity and increased resolution (Superose 6 Increase, n.d.). A protein mixture of small and large proteins is separated based on the particle migration. Larger proteins cannot enter the pores and result in eluting earlier (Hong, Koza, & Bouvier, 2012). Proteins that are smaller ultimately are retained in the beads longer and therefore elute last.

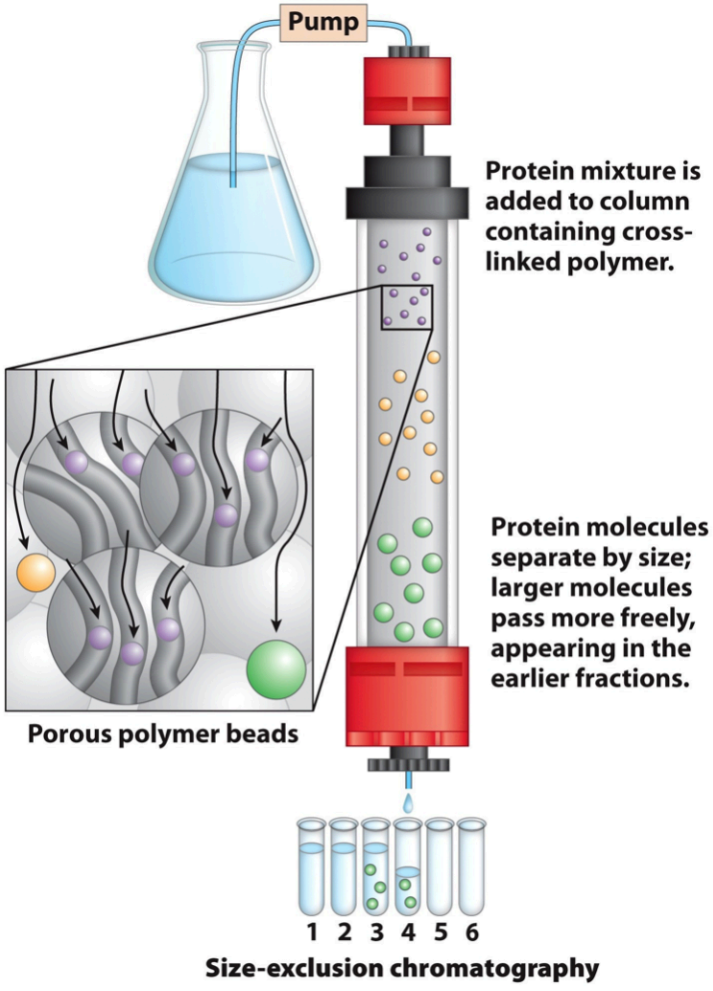

Figure 2.7 Size-exclusion column composed of porous polymer beads. Smaller proteins enter through these beads whereas proteins that are larger can pass through more freely, and elute earlier. Adapted from Lehninger Principles of Biochemistry, 6th Edition (Nelson & Cox, 2012).

In ion and size-exclusion columns, as the buffer continues to flow through the stationary phase, the fractions are collected while monitoring the conductivity and absorbance of the compounds eluted from the column over time, forming an elution curve or chromatogram. The resulting chromatogram is then analyzed to locate protein of interest. Each distinct peak is a representation of a unique component that may contain more than one protein species. Therefore, further analyses of the eluted fractions can be seen by an SDS-PAGE.

2.2.4 Sodium Dodecyl Sulfate Polyacrylamide Gel Electrophoresis (SDS)

SDS-PAGE is a technique used to separate proteins by size. The gel is commonly used for visualizing proteins molecular mass in kiloDalton (kDa), the abundance of major proteins in a sample, and the purity of the protein. This method uses a polyacrylamide gel as a support for migrating proteins and SDS along with a reducing agent (beta-mercaptoethanol) to denature proteins. The hydrophobic tail of the SDS denatures the structure of the complexed proteins making them into a linearized negatively charged protein. Also, beta-mercaptoethanol reduces the disulfide bonds of the protein, resulting in a destabilized structure.

The polyacrylamide gel has two different layers, the first layer known as the stacking layer that permits the protein samples to begin migrating at the same rate in time. The second layer or resolving layer responsible for separating the polypeptides by size. The linearized negative proteins always migrate towards the anode side that is positively charged in an electric field. Proteins with a higher molecular mass migrate slowly through the porous acrylamide gel compared to proteins that are smaller, which migrate faster through the gel.

2.3 Biophysical Analyses of Proteins

2.3.1 Circular Dichroism

Circular dichroism (CD) is a method used to understand the secondary structure of a protein in solution. The instrument (Figure 2.8A) is composed of an un-polarized light that is vibrating in more than one plane: horizontal, vertical, and side to side directions. The instrument also has a photoelastic modulator (PEM) that is an optical devise that modulates the polarized linear light (light moving in one direction: vertical or horizontal) to circular polarized light, meaning the light can travel in both circular directions, left-handed (counterclockwise) and right-handed (clockwise) (Circular Dichroism, 2014). As these two directions of light pass through the molecule, they begin to interact and the molecule may absorb right and left handed circularly polarized light to different extents (Greenfield, 2006). This interaction excites the molecule causing it to transition and rearrange. The remainder of light that is not absorbed will travel in the direction of a detector where the result is of different structural signatures (Figure 2.8B). A protein sample with alpha-helical structure have negative bands at 222 nm and 208 nm forming a “W” shaped signature and also have positive bands at 193 nm, disordered proteins emit a wavelength above 210 nm and negative bands near 195 nm. Proteins with well-defined antiparallel beta-pleated sheets have negative bands at 218 nm and positive bands at 195 nm (Greenfield, 2006). The difference in molar extinction coefficients for left and right-handed circularly polarized light ($\Delta\varepsilon$) is plotted as a function of wavelength within 190 and 250 nm (Nelson & Cox, 2012).

It is worth noting that CD spectroscopy is a good source for determining whether proteins are properly folded, estimating the fraction of secondary structure of the protein,

and monitoring transitions between folded and unfolded protein states (Nelson & Cox, 2012).

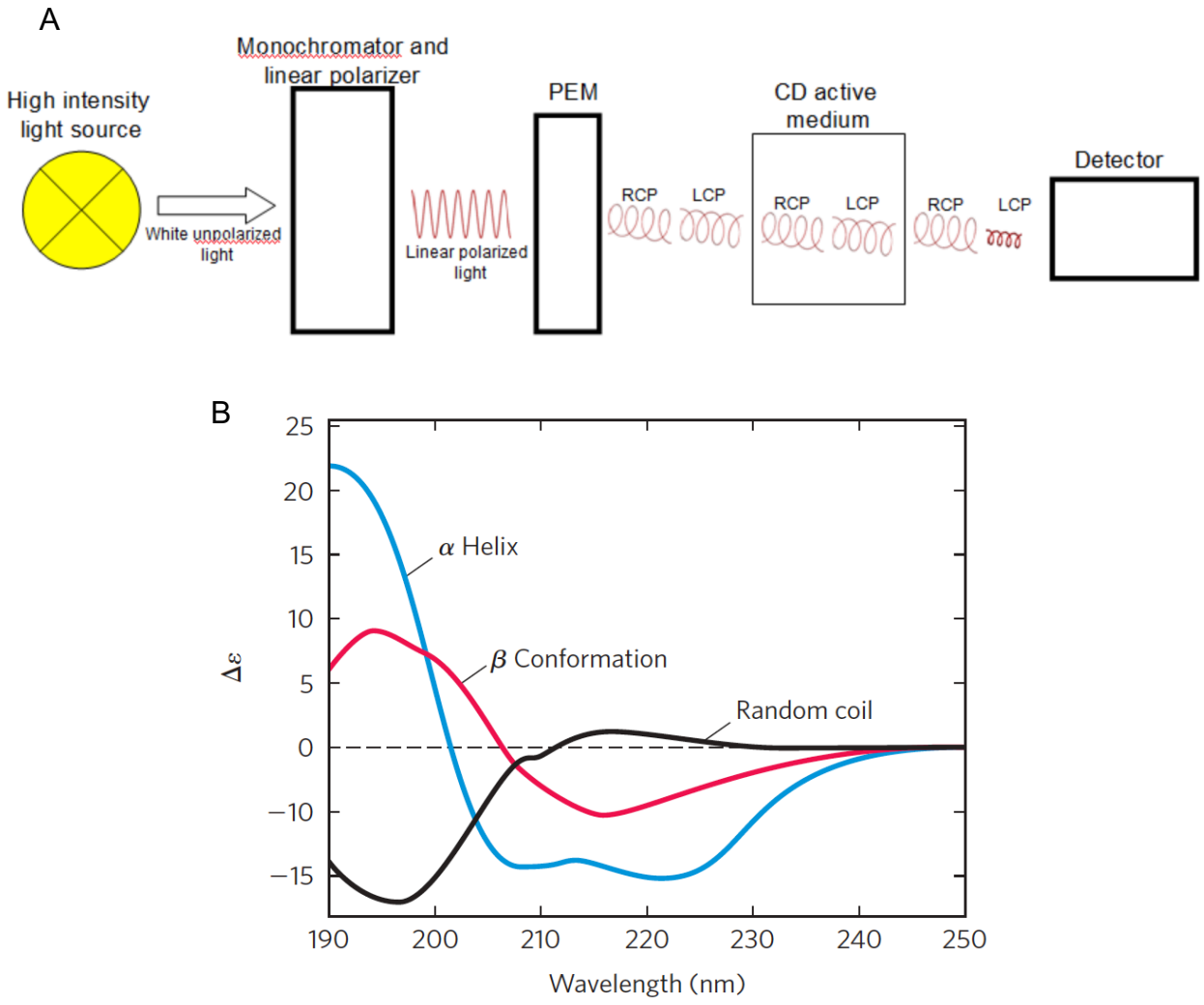

Figure 2.8 Instrumentation for CD spectrometer showing linear polarized light and the direction of right-handed circular polarized light and left-handed circular polarized light (A), the spectra showing different signatures of secondary structure (B). Adapted from Lehninger Principles of Biochemistry, 6th Edition (Nelson & Cox, 2012), and LibreTexts, Circular Dichroism (Circular Dichroism, 2017).

2.3.2 Dynamic Light Scattering

Dynamic light scattering (DLS) is a biochemical analysis that is often employed to measure the particle size distribution of a protein in solution. This method follows the Brownian motion, where particles in a solution result in different motions based on their thermal energy (Worldwide, 2011) (Figure 2.9). When the molecules are illuminated with a laser in this case a monochromatic laser, the intensity of the scattered light causes the molecules to move more rapidly (Worldwide, 2011). These results are mathematically translated into a size distribution or Gaussian curve (Figure 2.9). Not only is the particle size detected but the also the surface structure. In solution, the surface structure of the molecule can be made up of a single population of identical particles, also known as a monodisperse sample or two or more populations characterized as a polydispersed sample, or non-uniform size distribution. The different populations (monodisperse and polydisperse) are detected by a value known as polydispersity index (PDI). A PDI value less than 0.05 indicates a monodisperse protein and values above 0.7 indicates a polydisperse protein (Worldwide, 2011).

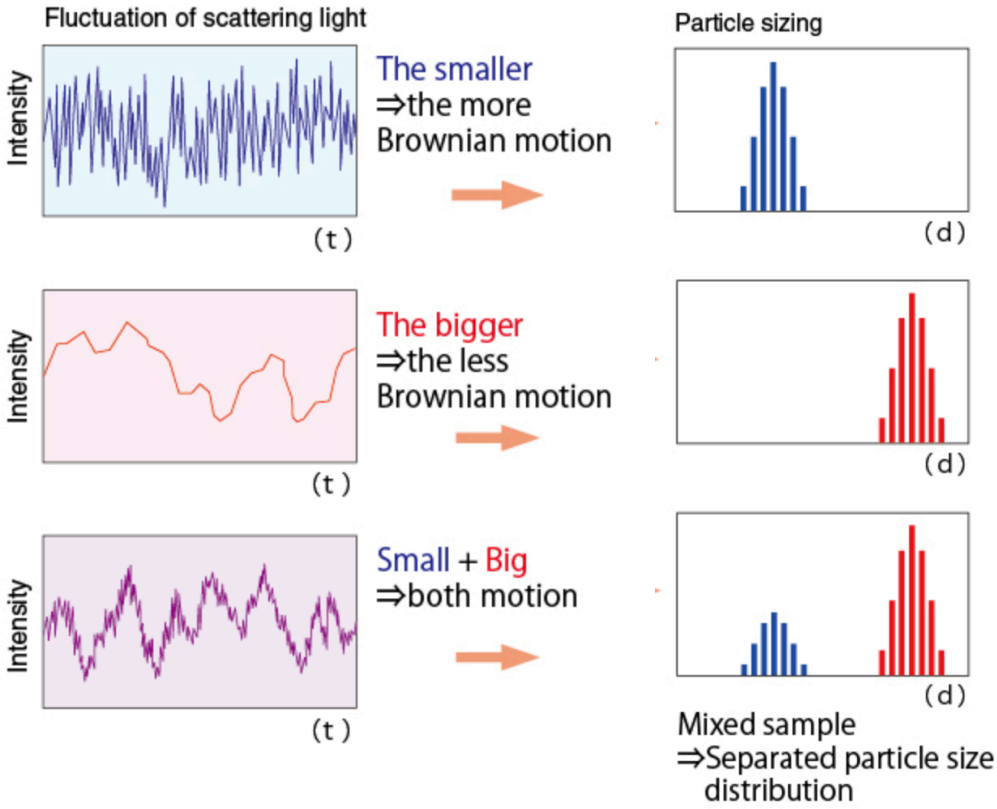

Figure 2.9 Represents the analysis of fluctuation of scattering light based on the size of the particle. Adapted from Otsuka, Principle of particle sizing: Dynamic Light Scattering Method (Dynamic Light Scattering Spectrophotometer DLS-8000 | Otsuka Electronics, n.d.).

2.4 Electron Microscopy

2.4.1 Instrumentation

A transmission electron microscope (Figure 2.10A) is an instrument designed for studying high resolution structures of viruses, organelles, and proteins. The microscope is a high vacuum cylindrical tube that is about 2 meters long. In the electron microscope, an electron beam hits the sample where the electrons interact with the atoms to form an image. The source of electrons is produced by thermo-ionic emitter that works like a light bulb. An accelerating voltage is applied to the surrounding cathode cap also known as

Wehnelt cylinder (Transmission Electron Microscopy, n.d.) (Figure 2.10B). A small emission current is then applied to a filament (cathode) where electrons are released. The change in negative voltage between the filament and the cathode cap creates an electron cloud (Transmission Electron Microscopy, n.d.). The electrons are rapidly moving due to the repulsion of the cathode cap. An anode located below the electron gun, attracts the negatively charged electrons where they accelerate through a channel where electromagnetic converging lenses are applied. The lenses are coils that surround the tube at different intervals. The electromagnetic field emitted by the coils causes the electrons to constrict and focus at the center of the sample (Transmission Electron Microscopy, n.d.) (Figure 2.10C). A condenser aperture controls the fraction of the beam that hits the sample, for controlling the intensity of illumination and preventing a blurry image. The specimen stage is located within the objective lens to magnify and focus the image. Below the stage, an objective aperture is used to enhance the contrast of the sample, as well as a projector lens to further magnify the image (Transmission Electron Microscopy, n.d.). The final result is the formation of an image composed of dark particles that are present on a white background.

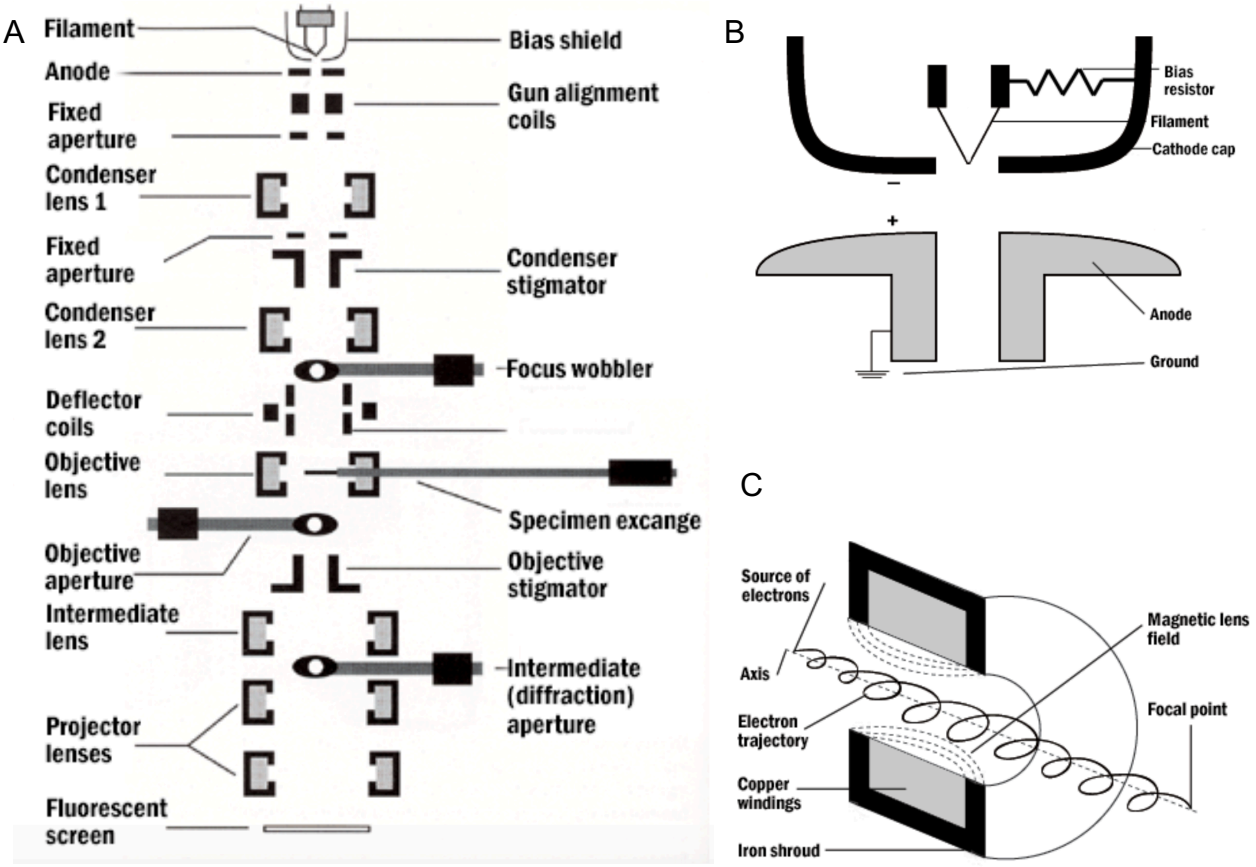

Figure 2.10 Set up of a transmission electron microscope (A). The set up of the electron gun for emission of electrons (B). The electron trajectory in a magnetic field lens (C). Adapted from the University of Iowa's Center for Microscopic Analysis (Transmission Electron Microscopy, n.d.).

2.4.2 Specimen Preparation for Negative Staining

Proteins and other biological molecules can be difficult for electron microscopy because of their sensitivity to radiation damage, poor capacity to scatter electrons, and prone to dehydration in the vacuum of the microscope (Ohi, Li, Cheng, & Walz, 2004). Therefore, the method for specimen preparation is considered when evaluating them under a microscope. The preparation of sample helps to prevent structural collapse of the protein and increase contrast. Negative staining is a method where the specimen is embedded in a layer of a dried heavy metal solution. This method was introduced as a

technique that allows for finer details of the molecules to be visualized due to the increase in contrast that comes from the interactions that occur between the electrons and the atoms of the heavy metals.

The sample to be imaged is prepared on a small grid (Figure 2.11). The grid is made up of a copper-coated film. A thin layer of sample is added on top of the carbon film. However, carbon is hydrophobic and any hydrophilic liquid that is layered above it will not interact. Therefore, to make the surface more accessible to the sample, the grid is placed under a high vacuum seal where glow-discharging is done resulting in a hydrophilic grid. When high voltage is applied this ionizes the gases within the chamber. The negative charged ions are deposited onto the copper-coated grid, resulting in a hydrophilic surface. Negative stains composed of heavy metals are added to the surface of the specimen to improve the amount of electrons that are absorbed. The most common stains are uranyl and tungstate stains. Each time the specimen is coated with a heavy metal stain, it is carefully blotted to remove any excess of stain (Ohi, Li, Cheng, & Walz, 2004). Removing the excess stain prevents unwanted artifacts that can appear in the imaging process. After staining, the specimen is ready to be examined under the microscope. In negative staining the particles of interest appear as white spots against a dark background.

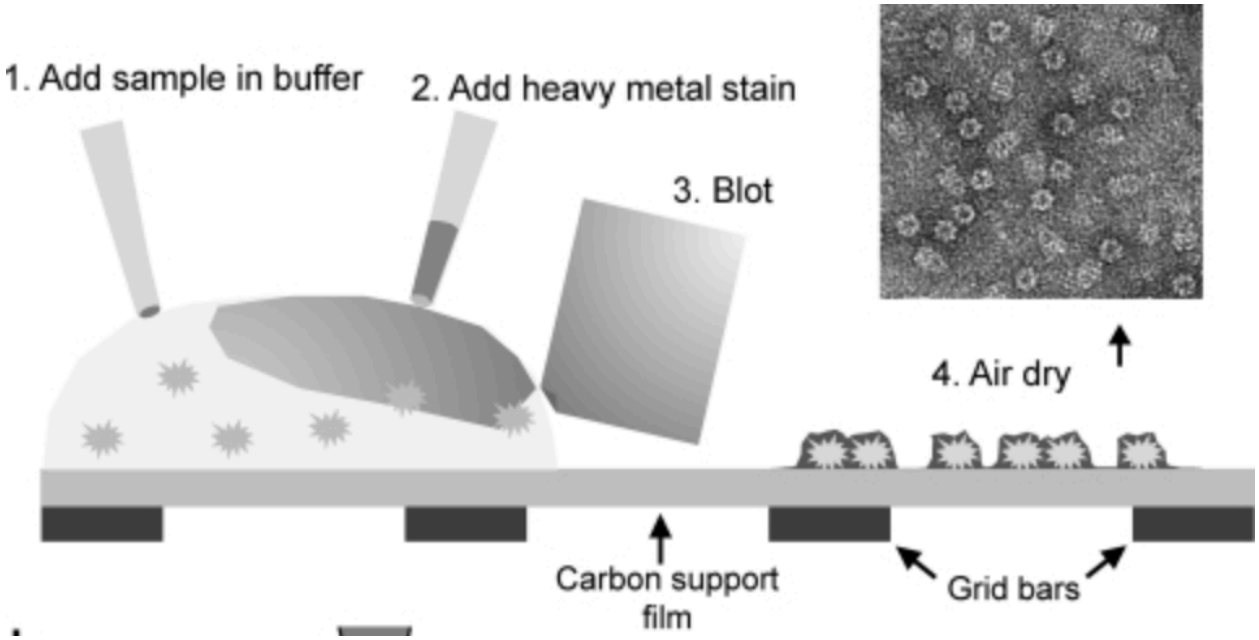

Figure 2.11 A schematic of specimen preparation: sample, negative stain composed of a heavy metal, blotting, and image formation. Adapted from Orlova, 2011 (Orlova, 2011).

Chapter 3: Experimental Approaches for Hsp27 and point mutation S135F

3.1 Cloning Heat Shock Protein 27

Primers were designed by obtaining the HSPB1 DNA sequence (ID: 3315) that encodes for Hsp27 protein from the National Center for Biotechnology Information website. The following sequence primers were designed and ordered from Integrated DNA Technologies (IDT):

Coding for Hsp27 WT

Forward 5' – TTT TCA TAT GAC CGA GCG CCG CGT CCC CTT CT – 3'

Reverse 5' – TTT TCT CGA GTT ACT TGG CGG CAG TCT CAT CGG – 3'

Coding for S135F point mutation in Hsp27 WT

Forward 5' - GGC TAC ATC TTC CGG TGC TTC – 3'

Reverse 5' – TGA AGC ACC GGA AGA TGT AGC C – 3'

Hsp27 WT was amplified in a 50 µl reaction that contained 0.5 µM of forward and reverse primers, 45 ng/µL of Hsp27 template, 1X of Phusion HF, 200µM of dNTP mix, and 1 unit/50µL Phusion DNA Polymerase. The reaction took place in a PCR machine from Prime Thermal Cycler. The reaction began as follows: initial denaturation at 98ºC for 30 seconds, followed by 30 cycles of DNA amplification that consisted of denaturation at 98ºC for 5 seconds, annealing at 65ºC for 5 seconds, elongation at 72ºC for 5 seconds with a final extension at 72ºC for 10 minutes. The PCR product was purified by using the protocol from QIAGEN QIAquick PCR Purification kit.

S135F was amplified by doing three separate PCR reactions where the third reaction would include the products from the first two PCR reactions. In the first PCR reaction, the following primers were used:

Forward 5' – TTT TCA TAT GAC CGA GCG CCG CGT CCC CTT CT – 3'

Reverse 5’ – TGA AGC ACC GGA AGA TGT AGC C – 3’

In the second PCR reaction, the following primers were used:

Forward 5’ - GGC TAC ATC TTC CGG TGC TTC – 3’

Reverse 5’ – TTT TCT CGA GTT ACT TGG CGG CAG TCT CAT CGG – 3’

Both reactions were set up in a total volume of 50 µl that included 0.5µM of forward and reverse primers, 45 ng/µL of Hsp27 template, 1X of Phusion GC Buffer, 200µM of dNTP mix, and 1 unit/50µL Phusion DNA Polymerase HD. The reaction began as follows: initial denaturation at 98ºC for 30 seconds, followed by 30 cycles of DNA amplification that consisted of denaturation at 98ºC for 5 seconds, annealing at 61ºC for 5 seconds, elongation at 72ºC for 5 seconds with a final extension at 72ºC for 10 minutes. The third PCR reaction consisted of 20 µL of each PCR product that was combined together with 200µM dNTP mix, and 1 unit/50 µL Phusion DNA polymerase HD. The final reaction began as follows: initial denaturation at 98ºC for 30 seconds, followed 30 cycles of denaturation at 98 ºC for 5 seconds, annealing at 67.05 ºC for 30 seconds, elongation at 72 ºC for 20 seconds with final extension at 72 ºC for 10 minutes. The PCR product was purified by following the protocol from QIAquick Gel Extraction and PCR Clean-up kit. 6 µls of the three reactions were loaded onto a .7% DNA agarose gel for analysis of product (Figure 3.1).

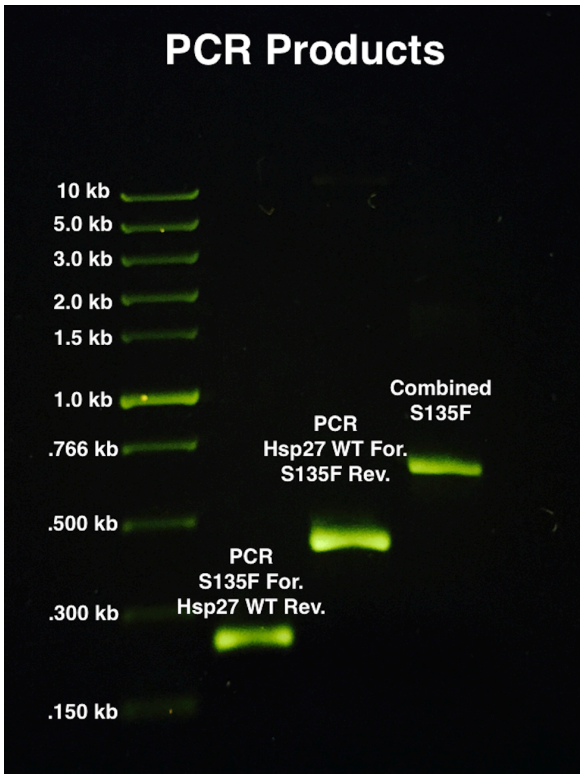

Figure 3.1 .7% agarose gel with PCR products of three reactions that were done to add the mutation S135F. The two PCR products were combined to obtained the final product with the mutation S135F. Sybr Safe from Invitrogen was used to stain the DNA and emit fluorescence when placed under blue light.

Double digestion was done by following the protocol from New England BioLabs (NEB) website. Two 50 µL reactions one with 1 µg of S135F DNA and the other with 1 µg of pET22 (b) that contained 1X Cut Smart buffer, 2 µl of NdeI and 2 µl of XhoI. Both digestions were set to incubate at 37 ºC for 2 hours, followed by inactivation at 65 ºC for 20 minutes. The digested product for S135F and pET22 (b) was cleaned up by following the protocol from NucleoSpin gel where a final concentration of S135F 110.5 ng/µl and pET22 (b) 2089.72 ng/µl was measured at an absorbance of 260nm with spectrophotometer. 6 µl of DNA and plasmid digestion were loaded onto a .7% DNA agarose gel for analysis (Figure 3.2).

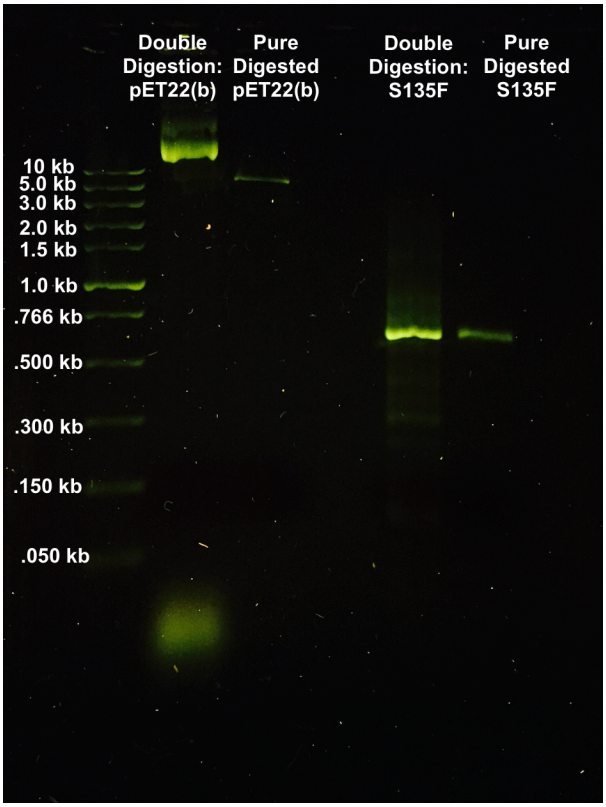

Figure 3.2 .7% agarose gel that contains the products of the before and after digested pET vector and S135F. Sybr Safe from Invitrogen was used to stain the DNA that emit fluorescence when placed under blue light.

Ligation of vector pET22 (b) with S135F was followed by using the protocol from New England BioLabs website. The reaction was set to a total volume of 14 µl with a ratio 1:4 of 16 ng/µl of gene and 14.5 ng/µl of plasmid with 7 µl of T4 DNA Ligase Master mix. The reaction was mixed by pipetting up and down 7-10 times and placed on ice where it was ready for bacterial transformation.

The obtained recombinant pETT22 (b)-HSPB1 was transformed into *E. coli* BL21(DE3) competent cells. The frozen competent cells were placed on ice until completely thawed out, followed by mixing 14 µl of pETT22 (b)-HSPB1 with cells and incubated on ice for 30 minutes. The mixture was moved to a water bath set to a

temperature exactly 42ºC for 10 seconds to allow the calcium chloride in the mixture to disrupt the cell membrane where pETT (b)-HSPB1 can enter. The mixture is moved back on ice for 5 minutes where it was mixed with 950 µl of SOC media that contains nutrients for cell growth. The cells were plated onto agar plates that contain nutrients for cell growth and 100 µg/ml ampicillin resistance for growth of only resistant colonies containing the cloned plasmid. The plates were moved to an incubator set to 37 ºC and left overnight. The colonies were then identified for the uptake of pETT22 (b)-HSPB1 through colony PCR (Figure 3.3).

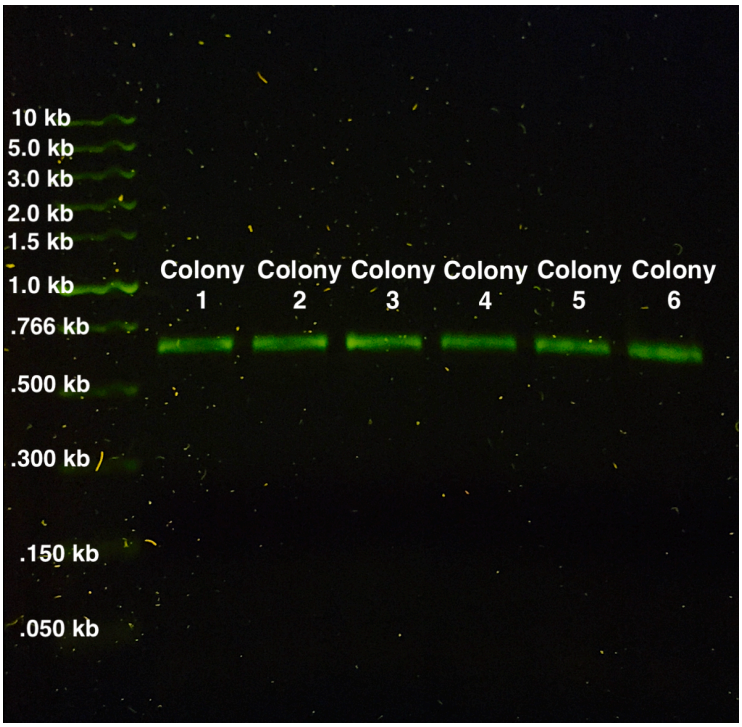

Figure 3.3 .7% agarose gel shows the colonies that have the DNA sequence S135F. Meaning that the cells were able to uptake pET22 (b) with HSPB1 mutation. Sybr Safe from Invitrogen was used to stain the DNA and emit fluorescence when placed under blue light.

Colonies 1-6 contained the pET22 (b)-HSPB1. pET22 (b)-HSPB1 expression were inoculated into a 100 mL baffled Erlenmeyer flask that contained 50 mLs of 2XTYmedia with 100 µg/ml of ampicillin. The cells were incubated in a shaker at 37ºC, at 220 rpm. After a few hours, the optical density (OD) for the cell reached .03-.4 at a wavelength of 600nm. This means that the cells were in their log phase or healthier. 25 mLs of the culture was mixed with 25 mLs of 50% glycerol diluted by 2XTY media. A total of 50 mLs were aliquoted into 1 mL eppendorfs for colonies 1-8 and stored in a -80 freezer for long term storage. The rest of the culture was left incubating until it reached an OD600 of .6-.8 where IPTG with a final concentration of 1mM was added for the induction of recombinant protein for 1 hour. A 10% SDS-PAGE was run for the analysis of the protein expression of the two colonies 5 and 7 (Figure 3.4A). Another 10% SDS-PAGE was run for the protein expression level for colonies 1-4, 6 and 8 (figure not shown). Colony 5 was picked for purification because it did not express protein of interest when no IPTG was added, that means that it did not have a leaky promoter (Figure 3.4B).

A

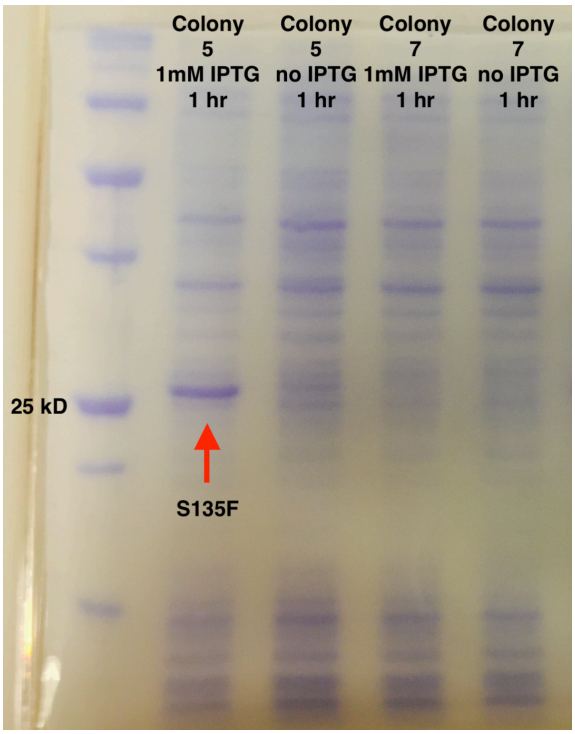

B

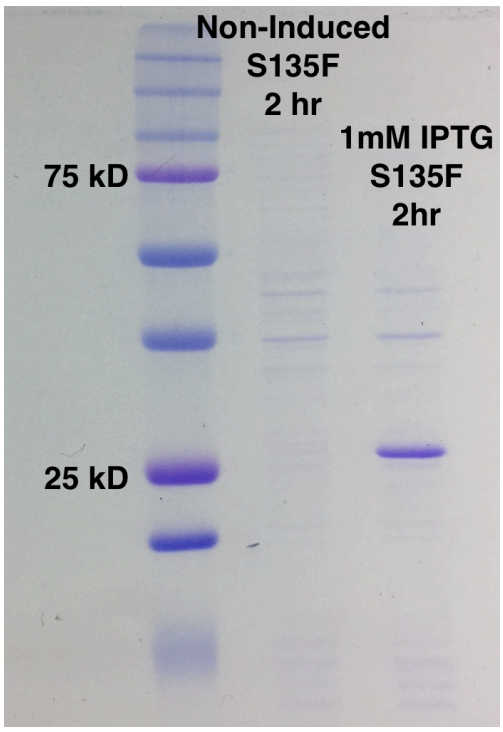

Figure 3.4 10% SDS-PAGE gel for testing protein expression with 1mM IPTG for 1 hour (A) 10% SDS-PAGE gel for protein expression with 1mM IPTG for 2 hours (B).

3.2 Optimization of Protein Expression Levels for Soluble Protein

Hsp27 was expressed at different concentrations of IPTG for increasing the amount of soluble protein. A culture was prepared by adding 100 µl of glycerol stock of Hsp27 WT into a 100 mL 2XTY with 100 µl of 100 µg/ml ampicillin and incubated at 37ºC. Once the OD600 reached between .6-.8, the 100 mL culture was divided into smaller cultures where 1mM and 4mM IPTG was added to each culture and checked every hour for a total time of 3 hours at 30ºC. 1 mL of culture was pipetted out and centrifuged where the pellet was re-suspended with 500 µl of DI water. The samples were loaded onto a 10% SDS-PAGE gel (Figure 3.5) for protein expression levels.

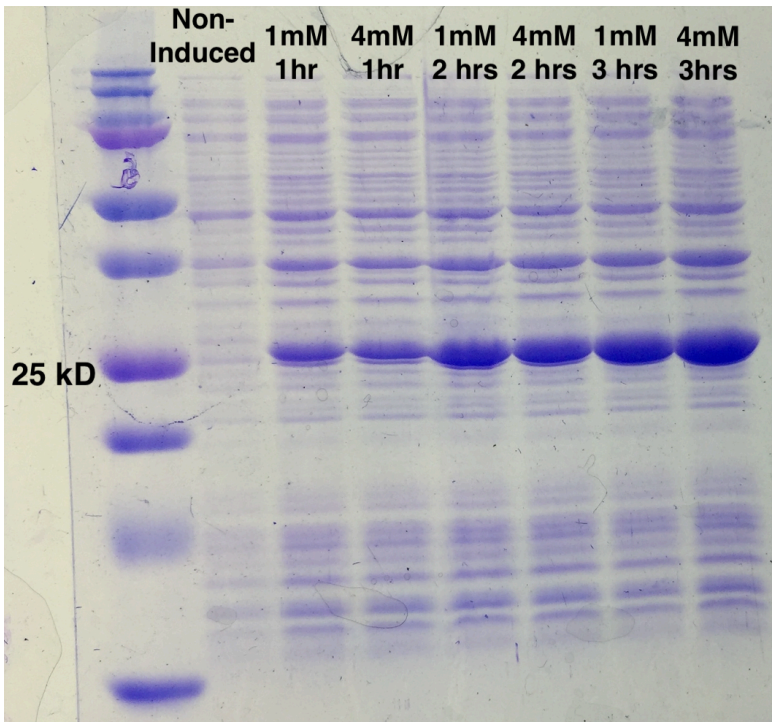

Figure 3.5 10% SDS-PAGE showing the amount of protein that is expressed when using different concentrations of IPTG over time at a temperature of 30ºC.

3.3 Cell Lysis

The cells were harvested by centrifugation at 6,000xg for 30 minutes at 4ºC. The cell pellet was re-suspended with lysis buffer (10 mMHepes pH 7.5, 5mM EDTA pH7.5), followed by the addition of 2mM PMSF and a pinch of Hen egg white lysozyme (Sigma, USA). The mixture was incubated in a Hula shaker at 4ºC for 1 hour to mix thoroughly. The mixture was then placed in a -20 freezer for initial freezing. Three cycles of freeze-thaws were applied to allow ice crystals to disrupt the cell membrane. The addition of 2mM PMSF was added after each thaw. The DNA was degraded by using the DNase I (Sigma, USA) and 60mM MgCl2. The mixture was placed in the Hula shaker for 30 minutes until the mixture became liquid. An addition of 3% of Streptomycin was added to the mixture and placed back in the Hula shaker for 30 minutes. The mixture was

centrifuged at 12,000xg for 30 minutes at 4ºC. The supernatant was transferred into a clean 50 mL tube where a gradient from 30% to 60% Ammonium Sulfate as a pre-purification step was added to locate the precipitated protein. A 10% SDS-PAGE was run for the analysis of precipitated protein at a different percentage of ammonium sulfate (Figure 3.6). The sample was mixed in the Hula shaker for 15 minutes and spun down at 12,000xg for 30 minutes at 4ºC. The recombinant protein remained in the 30% ammonium sulfate pellet where it was re-suspended with 2-4 mLs of chromatography buffer A (10mM Hepes pH 7.5, 5mM EDTA pH 7.5), until the solution appeared a tea-like color. 1 mL aliquots were stored in a -80 freezer for long term storage. The same procedure was followed for the mutation S135F.

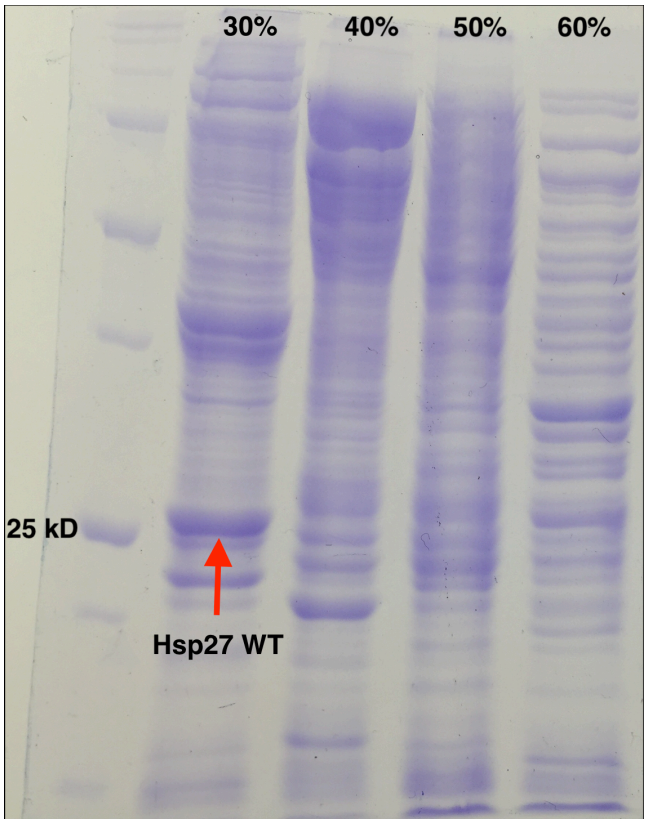

Figure 3.6 10% SDS-PAGE showing a gradient of ammonium sulfate at different concentrations to locate at which concentration Hsp27 precipitates.

3.4 Purification of Hsp27 and mutation S135F

The isoelectric point (pI) for Hsp27 was detected by adding the amino acid sequence onto ExPASy Bioinformatics Resource Portal website. The program revealed a theoretical pI of 5.98, that meant that it is composed of mostly negative charged amino acids at physiological pH 7.5. Therefore, the proteins were loaded onto an anion exchange column that contains positive charged immobilized groups. A column called HiTrap Q-XL from GE Healthcare Life Sciences was equilibrated first with 2 column volumes (CV) of chromatography buffer B (10 mMHepes pH 7.5, 5mM EDTA pH 7.5, 1M NaCl) then with 10 mLs of chromatography buffer A (10 mM Hepes pH 7.5, 5 mM EDTA

pH 7.5) at a flow rate of 5 mLs/min. 1 mL of crude protein was diluted in 20 mLs of chromatography buffer A (10mM Hepes, 5mM EDTA) and loaded through the sample pump to travel in the column at a flow rate of 2 mLs/min. 2 CV of buffer A was passed through the column to washout unbound protein. After washing, the proteins eluted with a linear gradient starting at 0 NaCl to 1M NaCl in 10mM Hepes pH 7.5 and 5mM EDTA pH 7.5. A 12% SDS-PAGE was done for the location of Hsp27. Fractions containing Hsp27 protein were transferred into a 30,000kDa Vivaspin 6 centrifugal concentrator unit and spun down at 4,000xg at 4ºC until the sample was a total of 200 µls. The 200 µls were injected into an AKTA purifier and loaded into a size exclusion column, Superose 6 Increase from GE Healthcare Life Sciences. The column was pre-equilibrated with 1 CV of chromatography buffer A (10mM Hepes pH 7.5, 5mM EDTA pH 7.5, 100mM NaCl). Collected fractions were loaded to a 12% SDS-PAGE (shown in results section). The fractions that contained the protein of interest were pooled and concentrated via a 10,000kDa Vivaspin 6 centrifugal concentrator unit. A 12% SDS-PAGE of the protein was done to see the final purity of the combined fractions that were concentrated (shown in results section) by loading 1 µl of protein in 4 µl of 4x loading SDS buffer (40% Glycerol, 240 mM Tris/HCl pH 6.8, 8% SDS, 0.04% bromophenol blue, 5% beta-mercaptoethanol). A pierce BCA assay was conducted to measure the final concentration of the pure protein for further assays. The same procedure was reproduced for S135F.

3.5 Chaperone Activity Assay of Hsp27 and S135F

The concentration of the protein was measured by BCA (Bicinchoninic acid) assay with BSA (bovine serum albumin) protein standard at a wavelength of 562nm. The activity assay was done by following the protocol from Bumagina, 2010. To measure the

chaperone activity of Hsp27, alpha-lactalbumin from Sigma was used as the substrate when reduced by a reducing agent, Dithiothreital (DTT). A 50 µl reaction was prepared by adding .85mg/mL of alpha-lactalbumin (100mM sodium phosphate buffer, 300mM NaCl, 1mM EDTA pH 6.2) inside a Quartz cuvette. The reaction was initiated by the addition of 35mM DTT and the mixture was moved to a PASCO spectrophotometer where the temperature was controlled to 37ºC and the absorbance was measured every 2 seconds at a wavelength of 400nm. A 1:1 reaction of 50 µl was set up by the addition of 60µM alpha-lactalbumin and 60µM of chaperone Hsp27. The reaction was commenced with the addition of 35mM DTT. The control was set to include 60µM alpha-lactalbumin without chaperone, 35mM DTT was added. The mixture was moved to the spectrophotometer, where the absorbance was measured. The reaction was repeated at another concentration 100µM of chaperone and 100µM of substrate. The same set up reaction was done for the chaperone Hsp27 with the mutation S135F.

3.6 Negative Staining

3.6.1 Negative Staining Sample Preparation

The concentration of pure protein was measured via BCA assay. 2% heavy atom uranium and methyl amine tungstate solutions were prepared by dissolving each in 1 mL of water. The samples were vortexed to ensure the heavy metal salt dissolved in water. The resulting solution was centrifuged at 12,000xg for 10 minutes. Meanwhile, a 400-mesh copper was discharged for 30 seconds by using the PELCO easiGlow Glow Discharge Cleaning System from TED PELLA INC, USA. The purified protein was then diluted to a final concentration of .1 mg/mL with chromatography buffer A (10mM Hepes pH7.5, 5mM EDTA pH 7.5, and 100mM NaCl). Once the surface of the grid was

discharged, the grid was picked up with a sharp-end tweezer where 3 µl of protein was embedded onto the carbon coated side. The excess protein was blotted off with white filter paper angled at 45º. 3 µl of 2% methyl amine tungstate was added to the coated surface of the protein followed by blotting the excess sample with filter paper. This was repeated twice by using uranium to make sure the heavy metal solution covers the protein to protect it from ionizing and generating radicals that damage the protein.

3.6.2 Negative Staining Data

The sample was then imaged by Dr. Ricardo Bernal that used a JEOL 3200FS transmission electron microscope at 300,000V with an emission gun that releases electrons towards the sample.

3.7 Biophysical Analyses

3.7.1 Circular Dichroism (CD)

A BCA assay was done on pure protein sample to measure the concentration of the protein at a wavelength of 562nm. The protein was then diluted with chromatography buffer A (10mM Hepes, 5mM EDTA, 100mM NaCl) at different concentrations: 60µM, 100µM, and 200µM. 30 µl of diluted sample was spread onto a .1mm cuvette glass plate for 100µm path length. The sample was recorded with a circular dichroism spec from Jasco J 1500 at 4ºC every 1nm, between wavelength 190nm and 260nm. Several cycles were done to assess the dynamics of the protein's secondary structure. This was repeated by changing the temperature of CD: 5ºC, 25ºC, 37ºC, and 42ºC with a sample concentration of 100µM.

3.7.2 Dynamic Light Scattering (DLS)

A BCA assay was done to measure the concentration of the protein for dynamic light scattering analysis. The protein was diluted to .5mg/ml in 1 mL of Chromatography Buffer A (10mM Hepes, 5mM EDTA, 100mM NaCl). The sample was transferred into a 3 mL cuvette where it was placed inside a DLS machine from Malvern. The machine was set to do the following measurements at different temperatures: 5ºC, 25ºC, 37ºC, and 42ºC. The measurements were recorded every 2 seconds for a total of 40-100 cycles.

Chapter 4: Results, Discussion, and Conclusion

4.1 Purity Analyses of Hsp27 WT and S135F

Isolating the protein of interest through chromatography, is vital for the characterization of the structure and function. As mentioned in chapter 1, Hsp27 is composed of different sizes, resulting to its unique functions in cells. Here, we isolated the bigger complex of Hsp27 to study its primary function as a chaperone.

Hsp27 WT was expressed at a higher temperature for 3 hours. The protein was loaded onto the ion-exchange followed by size-exclusion column. The fractions B8-B10 had the protein of interest, however, the chromatogram (figure not shown) showed an absorbance of 15 mAU, meaning there was not enough protein for the use of assays. Due to this, the protein was induced at a lower temperature and expressed for 20 hours with .1mM IPTG. The cell extraction was still prepared as mentioned in Ch.3. The protein was purified through the ion-exchange followed by size-exclusion column. The new chromatogram (figure not shown) of Hsp27 WT showed an absorbance of 283 mAu indicating more protein for conducting assays. The fractions tube number B8-B12 were pooled and concentrated together by a concentrating unit. Expressing the protein at a lower temperature was improved for obtaining a higher concentration of soluble protein. The same was done for mutation S135F. The protein samples of Hsp27 WT and S135F were added to a 12% SDS-PAGE to confirm the purity of each (Figure 4.1 A & B).

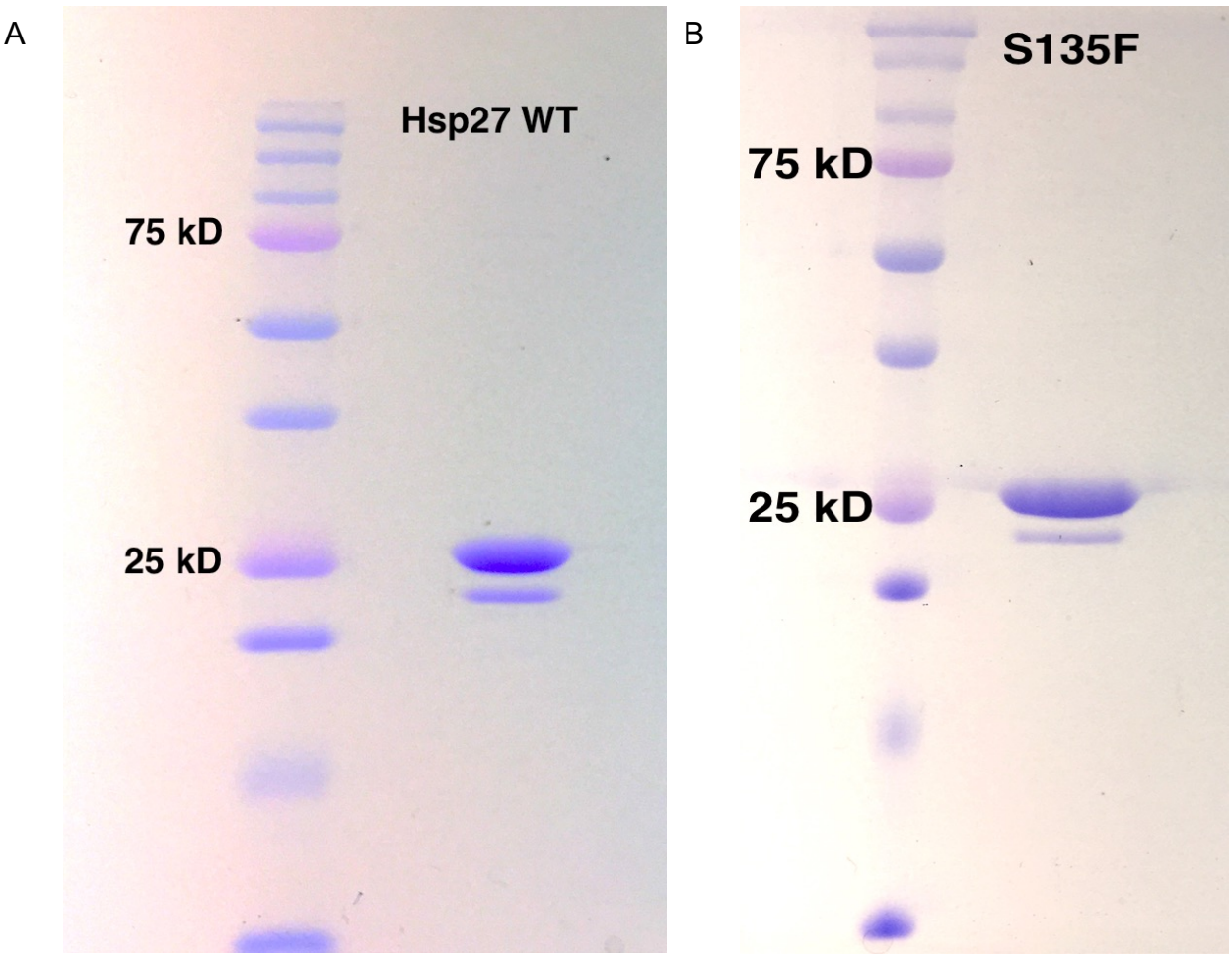

Figure 4.1 12% SDS-PAGE for concentrated fractions of Hsp27 WT (A) and S135F (B) after a two-column purification, ion-exchange followed by size-exclusion column.

4.2 Chaperone Activity for mutation S135F compared to Hsp27WT

In this assay, we wanted to study the primary function of chaperone Hsp27 WT and the mutation S135F involved in CMT, at normal human body temperature 37ºC. We used alpha-lactalbumin as a substrate for Hsp27. Based on the size-exclusion column, the larger complex of Hsp27 WT was able to protect misfolded alpha-lactalbumin that was induced by the addition of DTT (Figure 4.2A). These results were interesting because other papers (Rogalla, et al.) (Lelj-Garolla, 2006) (Panasenko, Seit Nebi, Bukach, Marston, & Gusev, 2002) were not clear in which small or large complex of Hsp27 is the active chaperone function. In these results, we confirmed that the larger complex is the active chaperone *in vitro*.

In the chaperone assay for S135F mutation in Hsp27, we saw that it protected alpha-lactalbumin for about 4 minutes, but the absorbance started to increase up to 1.5 mAu (Figure 4.2A). It was observed that the absorbance increased much higher than the control that was alpha-lactalbumin with 35mM DTT. This was interesting to see because previous papers had published that the mutation S135F had high chaperone activity (Almeida-Souza, et al., 2010). However, that statement was not clear in whether it protected the client protein from aggregating or the chaperone would bind tightly to the protein when misfolded. Based on this result, a 12% SDS-PAGE was done to analyze the precipitated sample to locate if S135F was precipitating with the substrate. The SDS-PAGE (Figure 4.2B) shows that S135F is in the pellet in the presence of alpha-lactalbumin, meaning that its chaperone properties is that it binds tightly to the client protein and precipitating with it. To make sure that DTT was not inducing the aggregation of S135F, a control where S135F and DTT without substrate was followed (Figure 4.3).

The results confirmed that DTT is not inducing the aggregation of S135F but instead S135F cannot protect misfolded protein, leading to both aggregating and precipitating.

A

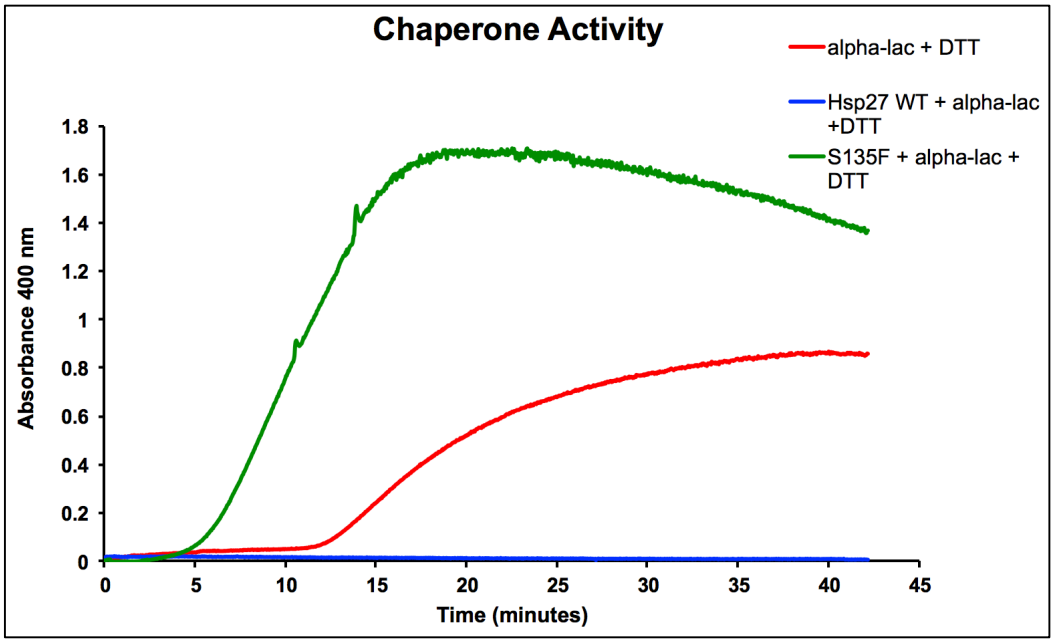

B

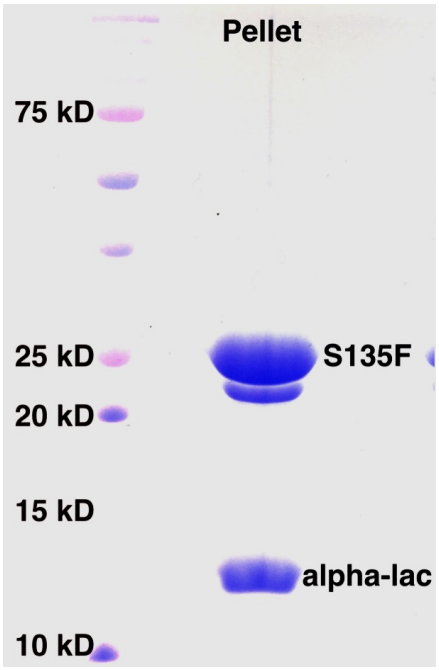

Figure 4.2 Red line indicates the control where no chaperone is added. Green line represents chaperone activity for mutation S135F with alpha-lac. Blue line indicates the chaperone activity of wild-type with alpha-lac (A). 12% SDS-PAGE gel showing the pellet of the precipitated proteins from the chaperone assay (B).

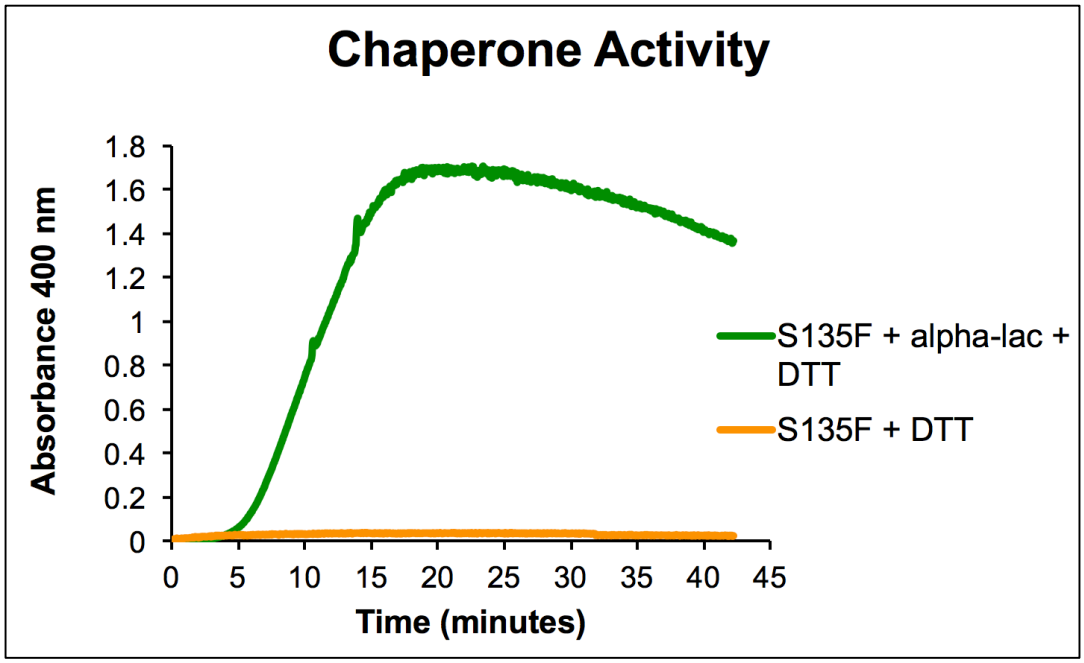

Figure 4.3 Green line represents the chaperone activity for mutation S135F. Orange line indicates the chaperone S135F with DTT only.

4.3 Secondary Structure of mutation S135F and Hsp27 WT

Hsp27 WT and mutation S135F showed different chaperone functions. Hsp27 WT can protect misfolded protein from aggregating unlike S135F that binds to the misfolded protein and completely aggregates. Because the chaperone activity assay for Hsp27 WT and mutation S135F are different, that must mean the structure is also different. To study the structural change between wild-type and the mutation, we did circular dichroism.

Published data reported that the structure of Hsp27 is concentration dependent, meaning that the structure changes at different concentrations (Shashidharamurthy, 2005). We first measured the secondary structure of Hsp27 WT and S135F at the concentration of 60μM based on the chaperone activity assay. Other concentrations, 100μM and 200μM were measured to see if the structure changed. The results showed that the secondary structure was composed of a mixture between beta sheet and alpha helix. It also showed that at different concentrations the secondary structure remained the same meaning the structure of Hsp27 WT and S135F did not change. Interestingly, S135F (Figure 4.4A) appeared to have more structure than the wild-type (Figure 4.4B) at 60μM or at any of the other concentrations measured.

A

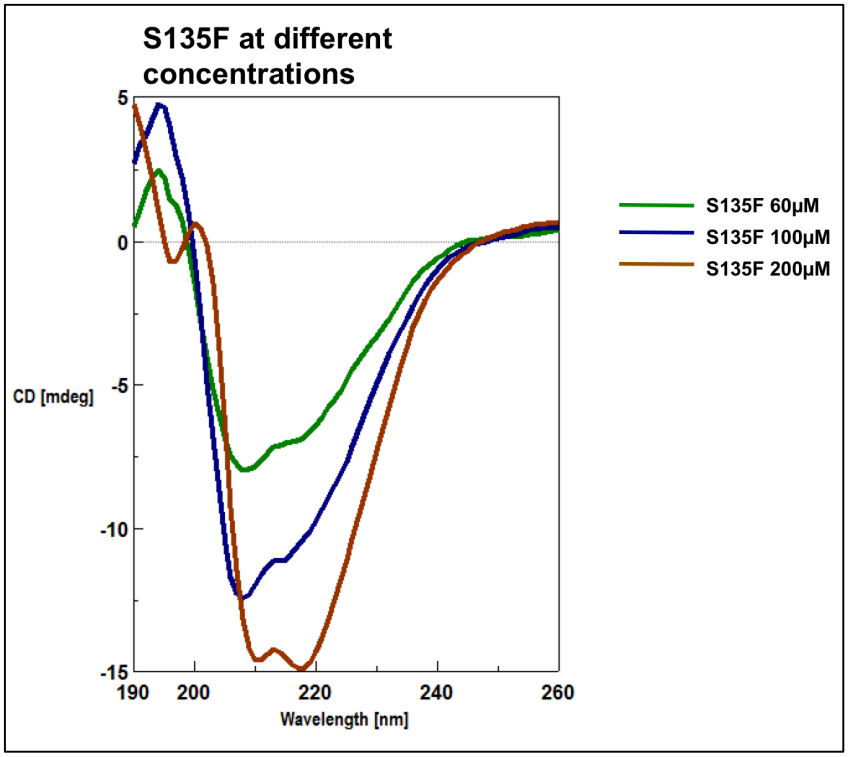

B

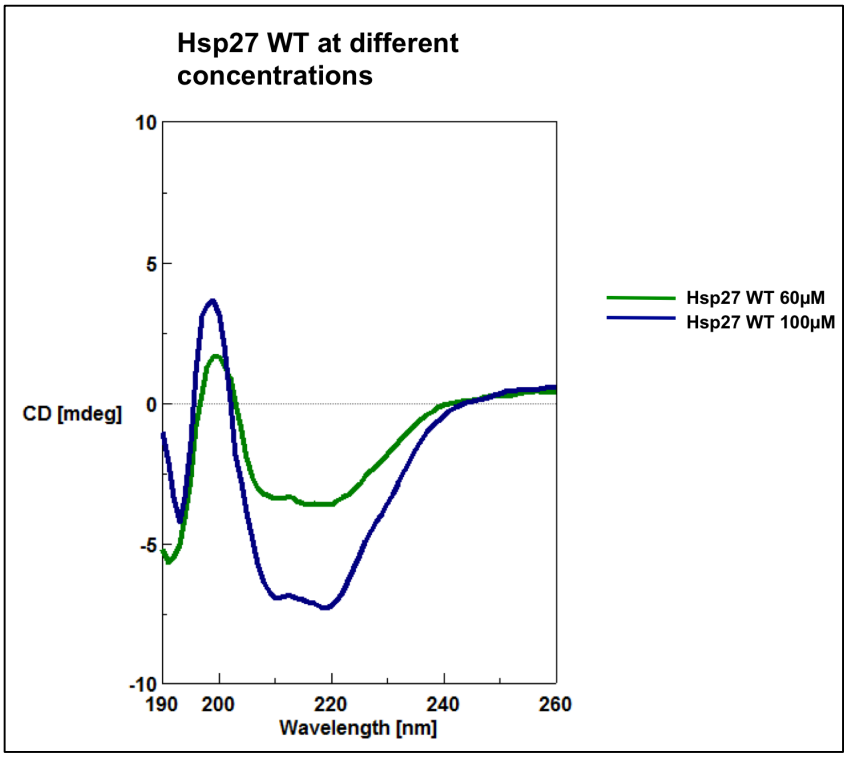

Figure 4.4 Green line represents the secondary structure of S135F at 60µM. Blue line indicates the secondary structure at 100µM. Brown line indicates secondary structure at 200 µM (A). Green line shows the secondary structure of Hsp27 WT at 60µM. Blue line indicates the secondary structure at 100µM (B).

Hsp27 is a heat shock protein, that is induced at different conditions at the cellular level (e.g. temperature change). We did a gradient of different temperatures to simulate heat shock: 5ºC, 25ºC, 37ºC, and 42ºC to study how these changes affect the secondary structure. At a concentration of 100μM for mutation S135F (Figure 4.5A) and Hsp27 WT (Figure 4.5B) mutation, interestingly their secondary structure changed. The structure of Hsp27 that is changed under heat shock conditions, implies that it is one of the many reasons why it is responsible for achieving and maintaining protein folding under stress conditions.

A

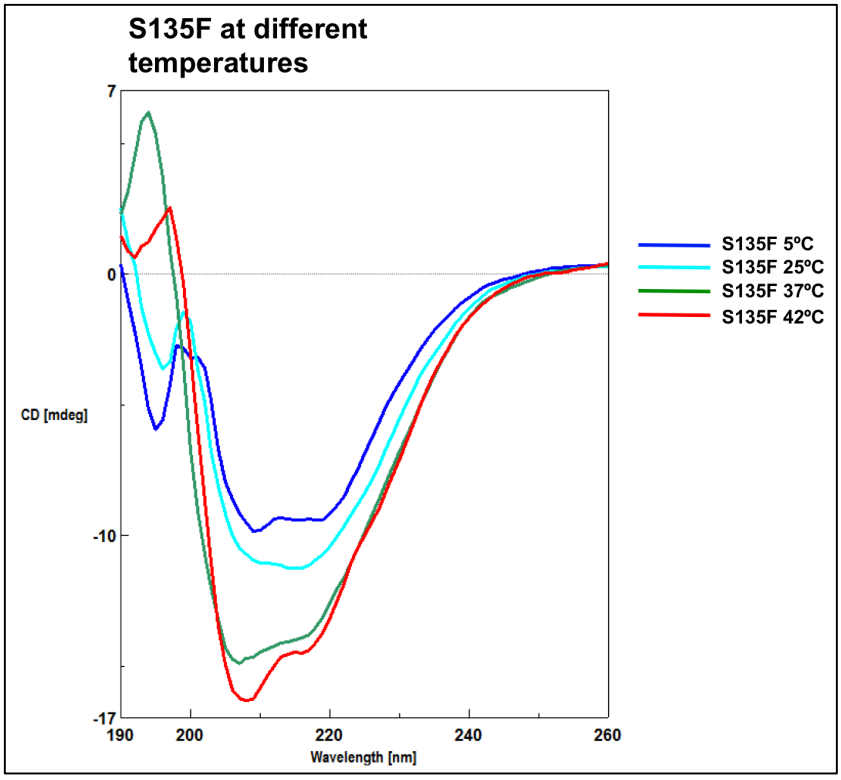

B

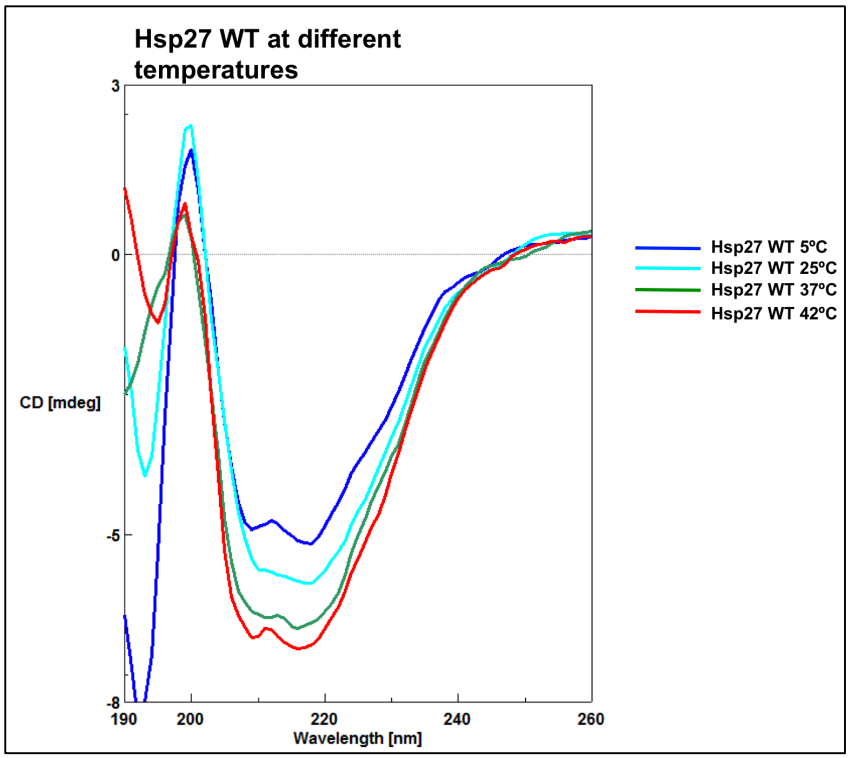

Figure 4.5 Blue line is the secondary structure of S135F at 5ºC. Light blue line indicates at 25ºC. Green line indicates at 37ºC. Red line indicates at 42ºC (A). Blue line is the secondary structure of Hsp27 WT at 5ºC. Light blue line indicates at 25ºC. Green line indicates at 37ºC. Read line indicates at 42ºC (B).

4.4 Size Characteristics of Hsp27 WT and S135F Chaperone

Dynamic light scattering as mentioned in chapter 2, is a method for measuring the size distribution of any particle. We used this method to measure the overall size distribution and the dispersity of Hsp27 WT and S135F in an aqueous environment at different temperatures. Both samples as mentioned in chapter 3 were prepared by diluting the protein to .5mg/ml in 1 mL of Buffer A (10mM Hepes, 5mM EDTA, 100mM NaCl). The DLS machine read the sample twice for a total of 92 readings.

Hsp27 WT was placed inside the DLS machine where the first temperature was set to read at 25ºC (Figure 4.6). We saw a size distribution of 18.13 d. nm with a polydispersity index value of 0.143, meaning polydispersed sample. As the temperature was increased to 37ºC, and 42ºC, the size distribution increased and became more uniform. The temperature was then decreased to 5ºC, where interestingly the size distribution was higher than 25ºC but still disordered.

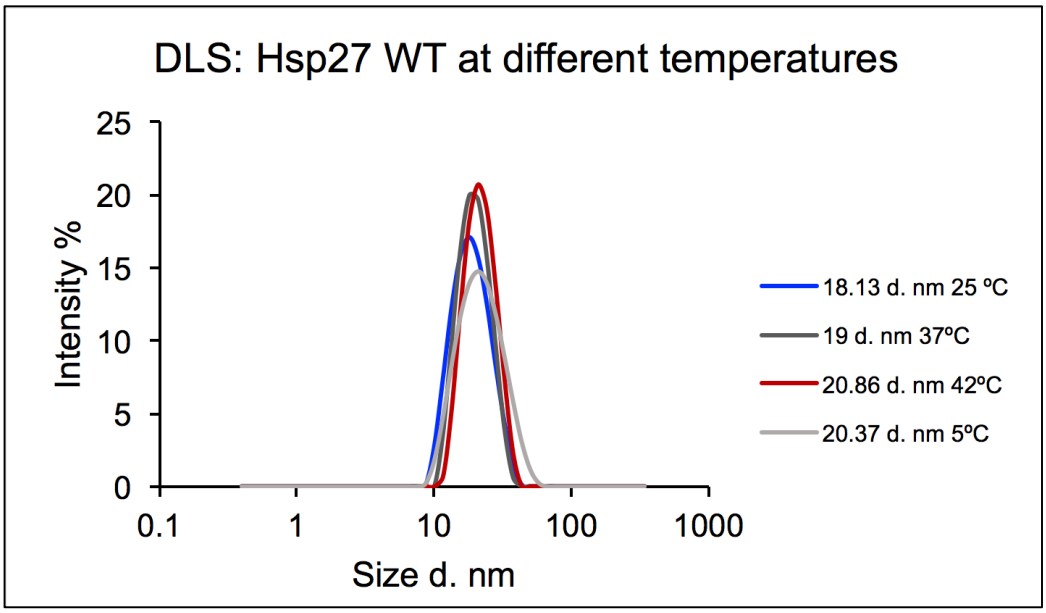

Figure 4.6 Blue line indicates the size distribution of Hsp27 WT at 25ºC. Dark grey indicates the size distribution at 37ºC. Red line indicates the size distribution at 42ºC. Light grey indicates the size distribution at 5ºC.

For the sample S135F the temperature was also changed, but this time as a gradient (Figure 4.7). The first reading at 5ºC showed a diameter of 17.62, smaller than the wild type chaperone Hsp27 at this temperature. However, based on the PDI it measured 0.070 meaning the protein was monodispersed. It also showed that as the temperature was increased the size distribution of the complexed increased significantly. At 42ºC the PDI was 0.004, meaning that the sample was very uniformed in subunit size. In comparison to the wild type it had more uniform symmetry because S135F had a PDI of 0.004 versus the wild type was 0.054. Also, the diameter size for S135F was 24.83 d. nm and Hsp27 WT was 20.86 d. nm. This is significant because it correlates with the previous data from CD that S135F has more secondary structure than the Hsp27 WT. The size distributions in Hsp27 under temperature changes appears to follow a subunit exchange mechanism that results in a uniform protein.

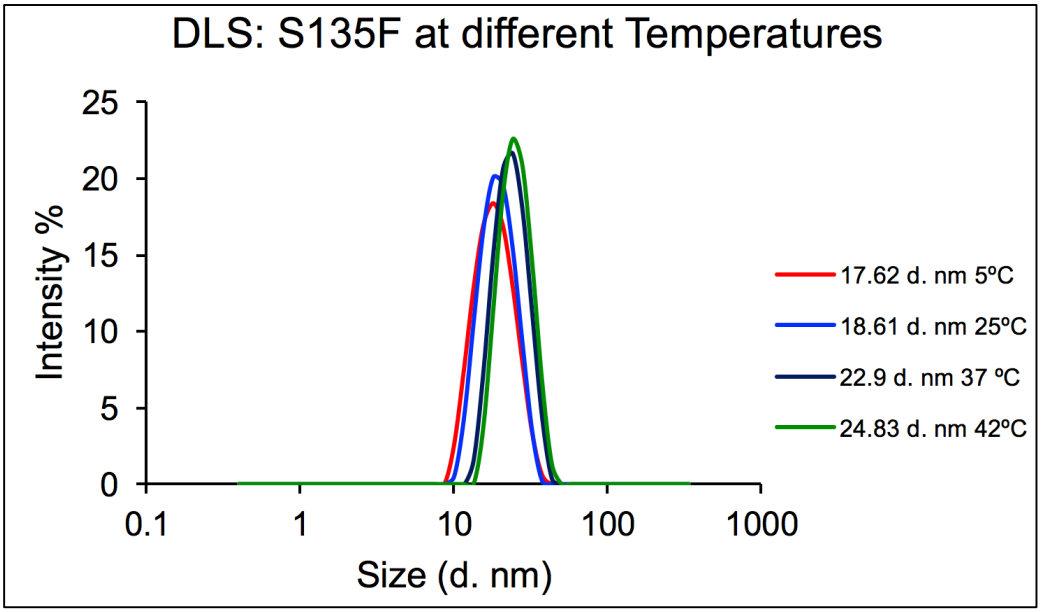

Figure 4.7 Red line indicates the size distribution of mutation S135F at 5ºC. Blue line indicates the size distribution at 25ºC. Black line indicates the size distribution at 37ºC. Green line indicates the size distribution at 42ºC.

4.5 Micrographs of Hsp27 WT and S135F

Through negative staining the mutation S135F showed that it was composed of small to large complexes (Figure 4.8). A reconstruction was intended but was not feasible because the mutation S135F did not have symmetry, therefore making it difficult to construct and image. This coincides with previous published work in that it is very difficult to obtain a structure of the heat shock protein 27 and its mutations. However, based on the DLS results, there is a possibility of incubating the protein sample at a temperature where the protein is symmetrical.

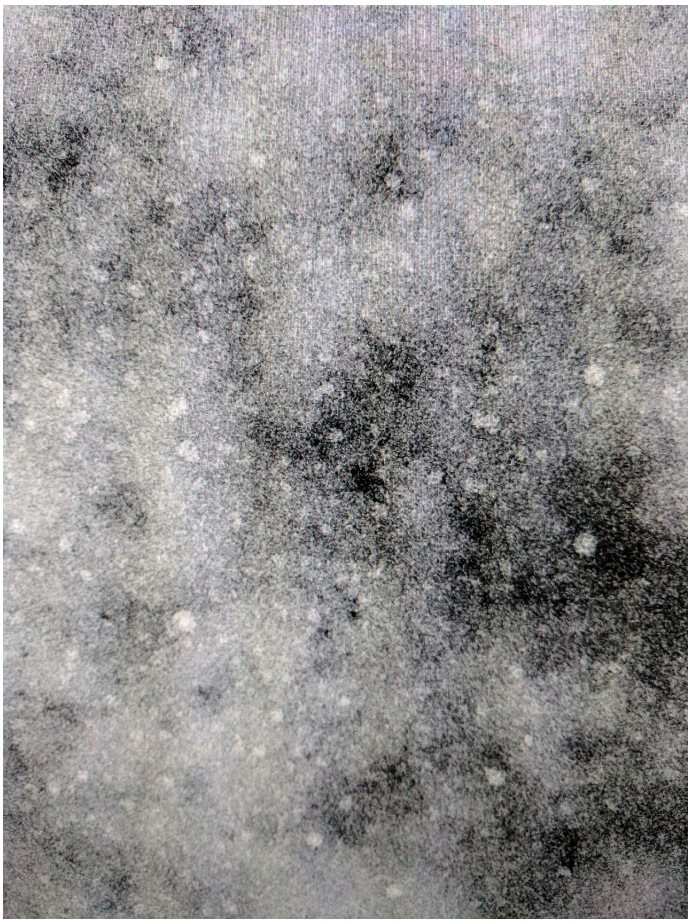

Figure 4.8 Negative stain image of S135F at .1 mg/mL from TEM.

4.6 Conclusion

Under regular and stress conditions, Hsp27 has the ability to change its oligomerization that are involved in many cellular functions important for the stability of the cells. To further investigate the properties of Hsp27 and its mutation S135F, 30% ammonium sulfate was added as a pre-purification step, followed by two purification columns, ion-exchange and size-exclusion chromatography. Based on the elution volume from the size-exclusion column, Hsp27 and S135F eluted as large oligomeric complexes. The chaperone activity was tested by using alpha-lactalbumin as a substrate for Hsp27 and S135F. It was observed that Hsp27 WT was able to prevent the substrate from aggregating in the presence of DTT, whereas the mutation could not protect the substrate. The mutation is located within the alpha-crystallin domain, which is already an unstable domain. In addition, the mutation's amino acid changes from a polar serine residue to phenylalanine, which is hydrophobic, is a potential for more instability as the polarity of serine may be relevant for substrate binding.

To further investigate the structure changes between the wild-type and the mutation, circular dichroism and dynamic light scattering were performed. As previously mentioned, the different concentrations did not play a factor in the structure change but did show that S135F was more structured than the wild-type. This is possibly one of the reasons S135F aggregates when bound to substrate. The structure of Hsp27 and S135F were highly influenced by changes in temperature. This relates back to small heat shock proteins being flexible in their structure under stress conditions. Negative stains were prepared to visualize the structure of the chaperone, however, because their size distribution changes rapidly, a single conformation cannot be isolated. There are other

alternatives (eg. computational analyses), however, a complete structure of Hsp27 WT and S135F remains unknown.

There are future directions that can help continue the biophysical analyses of Hsp27 and S135F. Since the conformations of Hsp27 WT and S135F change under different temperatures, it would be interesting to study the secondary structure changes when bound to misfolded substrate. DLS results indicated a change in size distribution that could be a way to isolate one confirmation of Hsp27 by incubating the protein at its favorable temperature before adding it onto a grid. In addition, studying different sizes of the wild-type and its mutation can help further understand their underlying mechanism involved in CMT. Previous studies reported that the smaller complex of Hsp27 provides better protection than bigger complexes, whereas others found no difference (Rogalla, et al.) (Lelj-Garolla, 2006) (Panasenko, Seit Nebi, Bukach, Marston, & Gusev, 2002). We found that the larger complex has chaperone properties as the wild-type was able to protect alpha-lactalbumin from aggregating. For mutation S135F, it was reported that it is a hyper-active chaperone *in-vivo*. Our results indicate that the large complexed S135 is hyper-active in terms of binding to the substrate and not able to protect from aggregation. The next step would be to study the chaperone activity of the smaller WT and S135F complexes through phosphorylation using MAPKAPK2 enzyme. Failure to protect the substrate could be one of the underlying causes of CMT.

Works Cited

6.5 High performance (high pressure) liquid chromatography (HPLC). (n.d.). Retrieved from http://elte.prompt.hu/sites/default/files/tananyagok/IntroductionToPracticalBiochemistry/ch06s05.html

Adams, J. (2008). *The proteome: discovering the structure and function of proteins.* Nature Education.

Alakomi , H. L., Saarela, M., & Helander, I. M. (2003). Effect of EDTA on Salmonella enterica serovar Typhimurium involves a component not asssignable to lipopolysaccharide release. *Microbiology*.

Alakomi, H. L., Paananen, A., Suihko, M. L., Helander, I. M., & Saarela, M. (2006). Weakening effect of cell permeabilizers on gram-negative bacteria causing biodeterioration. *Applied and Environmental Microbiology*, 4695-4703.

Alakomi, H. L., Saarela , M., & Helander, I. M. (2003). Effect of EDTA on Salmonella enterica serovar Typhimurium onvolves a competent not assignable to lipopolysaccharide release. *Microbiology* .

Alberts, B., Bray, D., Hopkin, K., Johnson, A., Lewis, J., Raff, M., & Walter, P. (2013). Unit 2: How Do Cells Decode Genetic Information into Functional Proteins? In *Essential cell biology.* Garland Science.

Almeida-Souza, L., Asselbergh, B., d'Y dewalle, C., Moonens, K., Goethals, S., Winter, V., . . . Janssens, S. (2011). Small heat-shock protein HSPB1 mutants stabilize microtubules in Charcot-Marie-Tooth Neuropathy. *Neurobiology of Disease*, 15320-15327.

Almeida-Souza, L., Goethals, S., de Winter, V., Dierick, I., Gallardo, R., Van Durme, J., . . . Janssens, S. (2010). Increased monomerization of mutant HSPB1 leads to protein hyperactivity in Charcot-Marie-Tooth neuropathy. *Journal of Biological*, 12778-12786.

Aquilina, A. J., Shrestha, S., Morris, A. M., & Ecroyd, H. (2013). Structural and Functional Aspects of Hetero-oligomers Formed by the Small Heat Shock Proteins alphaB-Crystallin and Hsp27. *The Journal of Biological Chemistry*.

Arrigo, A. P., & Gibert, B. (2012). HspB1 dynamic phospho-oligomeric structure dependent interactome as cancer therapeutic target. *Current Molecular Medicine*, 1151-1163.

Arrigo, A., Virot, S., Chaufour, S., Firdaus, W., Kretz-Remy, C., & Diaz-Latoud, C. (2005). Hsp27 Consolidates Intracellular Redox Homeostasis by Upholding Glutathione in Its Reduced Form and by Decreasing Iron Intracellular Levels. *Antioxidants and Redox Signaling*.

Bagnéris, C., Bateman, O. A., Naylor, C. E., Cronin, N., Boelens, W. C., Keep, N. H., & Slingsby, C. (2009). Crystal structures of alpha-crystallin domain dimers of alpaB-crystallin and Hsp20. *Journal of Molecular Biology*, 1242-1252.

Baranova, E. V., Weeks, S. D., Beelen, S., Bukach, O. V., Gusev, N. B., & Strelkov, S. V. (2011). Three-dimensional structure of alpha-crystallin domain dimers of human small heat shock protein HSPB1 and HSPB6. *Journal of Molecular Biology* .

Benndorf, R., Hayess, K., Ryazantsev, S., Wieske, M., Behlke, J., & Lutsh, G. (1994). Phosphorylation and supramolecular organization of murine small heat shock

protein HSP25 abolish its actin polymerizatio-inhibiting activity. *Journal of Biological Chemistry*.

Block, S. S. (2001). Antimicrobial Activity and Resistance . In *Disinfection, Sterilization, and Preservation* (p. 39). Philadelphia.

Bukau, B., & Horwich, A. L. (1998). The Hsp70 and Hsp60 chaperone machines. *Cell*, 351-366.

Bumagina, Z. M. (2010). Mechanism of suppression of dithiothreitol-induced aggregation of bovine α-lactalbumin by α-crystallin. *Biophysical chemistry*, 108-117.

Caetano-Anollés, G., Wang, M., Caetano-Anollés, D., & Mittenthal, J. E. (2009). The origin, evolution and structure of the protein world. *Biochemical Journal*.

Calderwood, S. K., Khaleque, M. A., Sawyer, D. B., & Ciocca, D. R. (2006). Heat shock proteins in cancer: chaperones of tumorigenesis. *Trends in Biochemical Sciences*, 187-196.

Charcot-Marie-Tooth Disease (CMT). (2017). Retrieved from MDA: https://www.mda.org/disease/charcot-marie-tooth

Charcot-Marie-Tooth Disease (CMT). (2017, November 29). Retrieved from MDA: https://www.mda.org/disease/charcot-marie-tooth

Charcot-Marie-Tooth Disease Fact Sheet. (n.d.). Retrieved from National Institute of Neurological Disorders and Stroke: https://www.ninds.nih.gov/Disorders/Patient-Caregiver-Education/Fact-Sheets/Charcot-Marie-Tooth-Disease-Fact-Sheet

Charette, S. J., & Landry, J. (2000). The interaction of HSP27 with Daxx identifies a potential regulatory role of HSP27 in Fas-induced apoptosis. *Annals of the New York Academy of Sciences*, 126-131.

Charette, S. J., Lavoie, J. N., Lambert, H., & Landry, J. (2000). Inhibition of Daxx-mediated apoptosis by heat shock protein 27. *Molecular and Cellular Biology* , 7602-7612.

Chung, K. W., Kim, S., Cho, S. Y., Hwang, S. J., Park, S. W., Kang, S. H., . . . Choi, B. (2008). Distal hereditary motor neuropathy in Korean patients with a small heat shock protein 27 mutation. *Experimental and Molecular Medicine* , 304-312.

Ciocca, D. R., Oesterreich, S., Chamness, G. C., McGuire, W. L., & Fuqua, S. A. (1993). Biological and clinical implications of heat shock protein 27,000 (Hsp27). *Journal of the National Cancer Institute*, 1558-1570.

Circular Dichroism. (2014, January 22). Retrieved from LibreTexts: https://chem.libretexts.org/Core/Physical_and_Theoretical_Chemistry/Spectroscopy/Electronic_Spectroscopy/Circular_Dichroism

Circular Dichroism. (2017, July 21). Retrieved from LibreTexts: https://chem.libretexts.org/Core/Physical_and_Theoretical_Chemistry/Spectroscopy/Electronic_Spectroscopy/Circular_Dichroism

Cummings, B. (n.d.). *From gene to protein*. Retrieved from http://www.bio.utexas.edu/faculty/sjasper/bio212/proteins.html

Dierick, I., Irobi, J., De Jonghe, P., & Timmerman, V. (2005). Small heat shock proteins in inherited peripheral neuropathies. *Annals of Medicine*, 413-422.

Dynamic Light Scattering Spectrophotometer DLS-8000 | Otsuka Electronics. (n.d.). Retrieved from Otsuka:

http://www.otsukael.com/product/detail/productid/23/category1id/2/category2id/2/category3id/32
Ehrnsperger, M., Lilie, H., Gaestel, M., & Buchner, J. (1999). The dynamics of Hsp25 quaternary structure. Structure and function of different oligomeric species . *Journal of Biological Chemistry*.
Ellis, R. J. (1987). Proteins as molecular chaperones. *Nature*, 378-379.
Ellis, R. J. (1993). Phil. Trasn. Biol. Sci.
Ellis, R. J., & Hemmingsen, S. M. (1989). Trends Biochem. Sci.
Engelking, L. R. (2015). Chapter 4 - Protein Structure. In *Textbook of Veterinary Physiological Chemistry* (Vol. III, pp. 18-25). Academic Press.
Evgrafov, O., Mersiyanova, I., Irobi, J., Bosch, L. V., Dierick, I., Leung, C. L., . . . Timmerman, V. (2004). Mutant small heat-shock protein 27 causes axonal Charcot-Marie-Tooth disease and distal hereditary motor neuropathy. *Nature Genetics*, 602-606.
Evstigneeva, Z. G., Solov'eva, N. A., & Sidel'nikova, L. I. (2000). Structures and Functions of Chaperones and Chaperonins (Review). *Applied Biochemistry and Microbiology*.
Fast protein liquid chromatography . (n.d.). Retrieved from Bio Rad : http://www.bio-rad.com/en-us/applications-technologies/fast-protein-liquid-chromatography
Fontaine, J. M., Rest, J. S., Welsh, M. J., & Benndorf, R. (2003). The sperm outer dense fiber protein is the 10th member of the superfamily of mammalian small stress proteins. *Cell stress and chaperones* , 62-69.
Fu, X. (2014). Chaperone function and mechanism of small heat-shock proteins. *Acta Biochimica et Biophysica Sinica*, 347-356.
Fuller, K. J., Issels, R. D., Slosman, D. O., Guillet, J. G., Soussi, T., & Polla, B. S. (1994). Cancer and teh heat shock response. *European Journal of Cancer*, 1884-1891.
Garrido, C., Bruey, J. M., Fromentin, A., Hamman, A., Arrigo, A. P., & Solary, E. (1999). Hsp27 inhibits cytochrome c-dependent activation of procaspase-9. *The FASEB Journal*, 2061-2070.
Giri, D. (2015, July 28). *Polymerase Chain Reaction (PCR) : Principle, Procedure, Components, Types and Applications*. Retrieved from LaboratoryInfo: http://laboratoryinfo.com/polymerase-chain-reaction-pcr/
Greenfield, N. J. (2006). Using circular dichroism spectra to estimate protein secondary structure. *Nature protocols*, 2876-2890.
Guay, J., Lambert, H., Gingras-Breton, G., Lavoie, J. N., Huot, J., & Landry, J. (1997). Regulation of actin filament dynamics by p38 map kinase-mediated phosphorylation of heat shock protein 27. *Journal of cell science*, 357-368.
Hartl, F. U. (1996). Molecular chaperones in cellular protein folding. *Nature*, 571-580.
Haslbeck, M. (2002). sHsps and their role in the chaperone network. *Cellular and Molecular Life Sciences*, 1649-1657.
Hohn, N., Hohn, D., Engel, A., Wurth, M., & Smith, P. R. (1979). *Mol. Biol., 129*, 359-373.
Hong, P., Koza, S., & Bouvier, E. (2012). Size-exclusion chromatography for the analysis of protein biotherapeutics and their aggregates. *Journal of liquid chromatography and related technologies*.

Huot, J., Houle, F., Spitz, D. R., & Landry, J. (1996). HSP27 phosphorylation-mediated resistance against actin fragmentation and cell death induced by oxidative stress. *Cancer research*, 273-279.

Introduction to size exlusion chromatography. (n.d.). Retrieved from Bio Rad : http://www.bio-rad.com/en-us/applications-technologies/introduction-size-exclusion-chromatography

Ion exchange chromatography. (n.d.). Retrieved from Bio Rad : http://www.bio-rad.com/en-us/applications-technologies/liquid-chromatography-principles/ion-exchange-chromatography

Katsogiannou, M., Andreieu, C., & Rocchi, P. (2014). Heat shock protein 27 phosphorylation state is associated with cancer progression. *Frontiers in Genetics*.

Laganowsky, A., Benesch, J. L., Landau, M., Ding, L., Sawaya, M. R., Cascio, D., . . . Eisenberg, D. (2010). Crystal structures of truncated alphaA and alphaB crystallins reveal structural mechanisms of polydispersity important for eye lens function. *Protein Science*, 1031-1043.

Langer, T., Lu, C., Echols, H., Flangan, J., Hayer, M. K., & Hartl, F. U. (1992). Successive action of Dnak, Dnaj and GroEL along the pathway of chaperone-mediated protein folding. *Nature*, 683-689.

Laskowska, E., Matuszewska, E., & Kuczyńska-Wiśnik, D. (2010). Small heat shock proteins and protein-misfolding diseases. *Current Pharmaceutical Biotechnology*, 146-157.

Lelj-Garolla, B. &. (2006). Self-association and chaperone activity of Hsp27 are thermally activated. *Journal of Biological Chemistry*, 8169-8174.

Linderstrøm-Lang, K., & Schellman, J. A. (1959). Protein structure and enzymatic activity. In *In The Enzymes* (pp. 443-510). New York : Academic Press.

Liquid chromatography principles. (n.d.). Retrieved from Bio Rad: http://www.bio-rad.com/en-us/applications-technologies/liquid-chromatography-principles

Marin-Vinader, L., Shin, C., Onnekink, C., Manley, J. L., & Lubsen, N. H. (2006). Hsp27 enhances recovery of splicing as well as rephosphorylation of SRp38 after heat shock. *Molecular Biology of the Cell*, 886-894.

McDonald, E. T., Bortolus, M., Koteiche, H. A., & Mchaourab, H. S. (2012). Sequence, structure, and dynamic determinants of Hsp27 (HspB1) equilibrium dissociation are encoded by the N-terminal domain. *Biochemistry*, 1257-1268.

Mehlen, P., Hickey, E., Weber, L. A., & Arrigo, A. P. (1997). Large unphosphorylated aggregates as the active form of hsp27 which controls intracellular reactive oxygen species and glutathione levels and generates a protection against TNFalpha in NIH-3 T3-ras cells. *Biochemical and Biophysical Research Communications*, 187-192.

Muchowski, P. J., Wu, G. J., Liang, J. J., Adman, E. T., & Clark, J. I. (1999). Site-directed mutations within the core 'alpha-crystallin' domain of the small heat-shock protein, human alphaB-crystallin, decrease molecular chaperone functions. *Journal of molecular biology*.

Mymrikov, E., Bukach, O. V., Seit-Nebi, A. S., & Gusev, N. B. (2010). The pivotal role of the beta 7 strand in the intersubunit contacts of different human small heat shock proteins . *Cell Stress Chaperones*, 365-377.

Nelson, D. L., & Cox, M. M. (2012). *Principles of Biochemistry* (Vol. Sixth Edition). New York : Lehninger.

Ohi, M., Li, Y., Cheng, Y., & Walz, T. (2004). Negative staining and image classification—powerful tools in modern electron microscopy. *Biological procedures online*.

Orlova, E. V. (2011). Structural analysis of macromolecular assemblies by electron microscopy. *Chemical reviews*.

Overview of cell lysis and protein extraction. (n.d.). Retrieved from ThermoFisher Scientific : http://www.thermofisher.com/us/en/home/life-science/protein-biology/protein-biology-learning-center/protein-biology-resource-library/pierce-protein-methods/overview-cell-lysis-and-protein-extraction.html

Panasenko, O. O., Seit Nebi, A., Bukach, O. V., Marston, S. B., & Gusev, N. B. (2002). Structure and properties of avian small heat shock protein with molecular weight 25 kDa. *Biochim. Biophys. Acta*, 64-74.

Pareyson, D., Marchesi, C., & Salsano, E. (2013). Dominant Charcot-Marie-Tooth syndrome and cognate disorders . In *Handbook of Clinical Neurology* (pp. 817-845).

Pauling, L., & Corey, R. B. (1951). The Polypeptide-chain configuration in hemoglobin and other globular proteins. *Proceedings of the National Academy of Sciences 37*, 443-510.

PET system manual. (n.d.). Retrieved from http://lifeserv.bgu.ac.il/wp/zarivach/wp-content/uploads/2017/11/Novagen-pET-system-manual-1.pdf

Protein structure . (2017, October 17). Retrieved from LibreTexts: https://bio.libretexts.org/LibreTexts/University_of_California_Davis/BIS_2A%3A_Introductory_Biology_(Britt)/Readings/Protein_structure

Rogalla, T., Ehrnsperger, M., Preville, X., Kotlyarov, A., Lutsch, G., Ducasse, C., . . . Gaestel, M. (n.d.). Regulation of Hsp27 oligomerization chaperone function, and protective activity against oxidative stree/tumor necrosis factor alpha by phosphorylation. *Journal of Biological Chemistry*.

Rosano, G. L., & Ceccarelli, E. A. (2014). Recombinant protein expression in Escherichia coli: advances and challenges. *Frontiers in microbiology*.

Schellman, J. A., & Schellman, C. J. (1997). Kaj Ulrik Linderstrøm-Lang (1896–1959). *Protein Science* .

Selkoe, D. J. (2004). Folding proteins in fatal ways. *Nature*.

Shashidharamurthy, R. K. (2005). Mechanism of Chaperone Function in Small Heat Shock Proteins DISSOCIATION OF THE HSP27 OLIGOMER IS REQUIRED FOR RECOGNITION AND BINDING OF DESTABILIZED T4 LYSOZYME. *Journal of Biological Chemistry*, 5281-5289.

Slavotinek, A. M., & Biesecker, L. G. (2001). Unfolding the role of chaperones and chaperonins in human disease. *Trends in Genetics Cell Press*, 528-535.

Sun, Y., & MacRae, T. H. (2005). The small heat shock proteins and their role in human disease. *The FEBS Journal*, 2613-2627.

Superose 6 Increase. (n.d.). Retrieved from GE Healthcare Life Sciences : http://www.gelifesciences.com/webapp/wcs/stores/servlet/catalog/en/GELifeSciences-us/products/AlternativeProductStructure_17418/29091596

Takeuchi, S. (2006). Analytical assays of human HSP27 and thermal-stress survival of Escherichia coli cells that overexpress it. *Elsevier*, 1252-1256.

Thériault, J. R., Lambert, H., Chávez-Zobel, A. T., Charest, G., Lavigne, P., & Landry, J. (2004). Essential role of the NH2-terminal WD/EPF motif in the phosphorylation-activated protective function of mammalian Hsp27. *Journal of Biological Chemistry*.

Traditional methods of cell lysis . (n.d.). Retrieved from ThermoFisher: https://www.thermofisher.com/us/en/home/life-science/protein-biology/protein-biology-learning-center/protein-biology-resource-library/pierce-protein-methods/traditional-methods-cell-lysis.html

Transmission Electron Microscopy. (n.d.). Retrieved from Central Microscopy The Univeristy of Iowa : https://cmrf.research.uiowa.edu/transmission-electron-microscopy

Transmission Electron Microscopy. (n.d.). Retrieved from Central Microscopy The University of Iowa: https://cmrf.research.uiowa.edu/transmission-electron-microscopy

Vaara, M. (1992). Agents that increase the permeability of the outer membrane . *Microbiology*.

Vidyasagar, A., Wilson, N. A., & Djamali, A. (2012). Heat shock protein 27 (HSP27): biomarker of disease and therapeutic drug. *Fibrogenesis & Tissue Repair*.

Vierling, E. (1997). The small heat shock proteins in plants are memebers of an ancient family of heated induced proteins. *Acta Physiologiae Plantarum*, 539-547.

Wilhelmus, M. M. (2007). Heat shock proteins and amateur chaperones in amyloid-Beta accumulation and clearance in Alzheimer's disease. *Molecular neurobiology*, 203-216.

Worldwide, M. I. (2011). *Dynamic light scattering, Common terms defined*. Retrieved from Inform white paper. Malwern Instruments Limited: http://www.biophysics.bioc.cam.ac.uk/wp-content/uploads/2011/02/DLS_Terms_defined_Malvern.pdf

Curriculum Vita

Janelly Villalobos was born on January 15th, 1992 to Maria De Lourdes Vasquez and Victor Villalobos in El Paso, Texas. Janelly Villalobos received her Bachelors of Science degree from the University of Texas at El Paso in December 2015. In Spring 2016, she joined the Master program in Environment Science Department of UTEP under the guidance of Dr. Ricardo Bernal. Where her curiosity and intellectual angst were fostered and developed through the structural and biological activity investigation of S135F mutation in Hsp27 involved in Charcot-Marie-Tooth disease.

Janelly Villalobos currently lives in El Paso where she plans to continue her education in medical school.

Email Address: janellyvillalobos@gmail.com